COMENIUS UNIVERSITY IN BRATISLAVA
FACULTY OF MATHEMATICS, PHYSICS
AND INFORMATICS

MATHEMATICAL MODELLING OF CELL DEATH IN PRESENCE OF SYNCHRONOUS INVASION OF TRICHINELLA SPIRALIS PARASITE

MASTER THESIS

2014 Bc. Jakub KOVÁCS

COMENIUS UNIVERSITY IN BRATISLAVA
FACULTY OF MATHEMATICS, PHYSICS AND INFORMATICS

MATHEMATICAL MODELLING OF CELL DEATH IN PRESENCE OF SYNCHRONOUS INVASION OF TRICHINELLA SPIRALIS PARASITE

MASTER THESIS

Study program:	Economics and Financial Mathematics
Study field:	9.1.9. Division of Applied Mathematics
Department:	Department of Applied Mathematics and Statistics
Supervisor:	Mgr. Richard Kollár, PhD.

Bratislava 2014 **Bc. Jakub KOVÁCS**

UNIVERZITA KOMENSKÉHO V BRATISLAVE
FAKULTA MATEMATIKY, FYZIKY A INFORMATIKY

MATEMATICKÉ MODELOVANIE BUNKOVEJ SMRTI V PRÍTOMNOSTI SYNCHRÓNNEJ INVÁZIE TRICHINELLA SPIRALIS

DIPLOMOVÁ PRÁCA

Študijný program:	Ekonomická a finančná matematika
Študijný odbor:	9.1.9. Aplikovaná matematika
Školiace pracovisko:	Katedra aplikovanej matematiky a štatistiky
Vedúci práce:	Mgr. Richard Kollár, PhD.

Bratislava 2014 **Bc. Jakub KOVÁCS**

Univerzita Komenského v Bratislave
Fakulta matematiky, fyziky a informatiky

ZADANIE ZÁVEREČNEJ PRÁCE

Meno a priezvisko študenta: Bc. Jakub Kovács
Študijný program: ekonomická a finančná matematika (Jednoodborové štúdium, magisterský II. st., denná forma)
Študijný odbor: 9.1.9. aplikovaná matematika
Typ záverečnej práce: diplomová
Jazyk záverečnej práce: slovenský

Názov: Matematické modelovanie bunkovej smrti v prítomnosti synchrónnej invázie Trichinella spiralis.

Cieľ: Navrhnutie modelu interakcií dôležitých pri programovanej bunkovej smrti (apoptóze) najmä za prítomnosti synchrónnej invázie parazita Trichinelly spiralis.

Vedúci: Mgr. Richard Kollár, PhD.
Katedra: FMFI.KAMŠ - Katedra aplikovanej matematiky a štatistiky
Vedúci katedry: prof. RNDr. Daniel Ševčovič, CSc.

Dátum zadania: 25.01.2013

Dátum schválenia: 04.02.2013 prof. RNDr. Daniel Ševčovič, CSc.
garant študijného programu

.....
študent

.....
vedúci práce

I declare this thesis was written on my own, with the only help provided by my supervisor and the referred literature.

Words of Thanks I would like to express special thanks to my supervisor Mgr. Richard Kollár, PhD. for all support and guidance he offered throughout the elaboration of this thesis and prof. MUDr. Pavel Babál, CSc. for his insightful meeting with us. I thank as well to all my teachers and professors, both from the program and those involved in my previous education. To all my friends and family, who supported me along my whole studies.

Abstrakt v štátnom jazyku

KOVÁCS, Jakub: Matematické modelovanie bunkovej smrti v prítomnosti synchrónnej invázie Trichinella spiralis [Diplomová práca], Univerzita Komenského v Bratislave, Fakulta matematiky, fyziky a informatiky, Katedra aplikovanej matematiky a štatistiky; školiteľ: Mgr. Richard Kollár, PhD., Bratislava, 2014, 68p.

Keď Trichinella spiralis nakazí svalovú bunku, spustí sa apoptóza, ktorá je kľúčovou zložkou všetkých vyšších organizmov. Pozostáva z komplexných vzťahov medzi bielkovinami a organelami v bunke. Matematické modelovanie pomáha analyzovať komplikované systémy ako tieto. V tejto práci sme zostrojili dva matematické modely apoptózy a pokúsili sme sa zahrnúť vplyv červa, ktorý po niekoľkých dňoch zastaví prebiehajúcu bunkovú smrť. Preto sme navrhli výmenu pôvodných mitochondrií za obmenené pomocou zmeny syntetizačných konštánt všetkých bielkovín, ktoré sa syntetizujú na alebo v mitochondriách. Naše simulácie odhalili, že i slabá zmena v činnosti mitochondrií má veľký dopad na proces bunkovej smrti.

Kľúčové slová: Apoptóza, Matematický model, Trichinella spiralis, Mitochondrie, Bistabilita

Abstract

KOVÁCS, Jakub: Mathematical Modelling of Cell Death in Presence of Synchronous Invasion of Trichinella Spiralis Parasite [Master Thesis], Comenius University in Bratislava, Faculty of Mathematics, Physics and Informatics, Department of Applied Mathematics and Statistics; Supervisor: Mgr. Richard Kollár, PhD., Bratislava, 2014, 68p.

When a muscle cell is infected by Trichinella spiralis, it triggers apoptosis. It is a key feature of all the higher organisms and consists of complex relations between proteins and organelles within a cell. Mathematical modelling helps to analyse such complicated systems. In this thesis, we constructed two mathematical models of apoptosis and tried to include the influence of the worm that after few days forces the ongoing cell death to cease. We, therefore, proposed substitution of original mitochondria for altered mitochondria by changing the synthesis rate of all apoptotic proteins synthesised inside or on mitochondria. Our simulations showed that even slight change in mitochondrial activity had a great impact on the process of cell death.

Keywords: Apoptosis, Mathematical model, Trichinella spiralis, Mitochondria, Bistability

Contents

List of Figures

Introduction

Apoptosis is the process of programmed cell death or cell suicide. It is a normal and regulated part of cell's life in a multicellular organism. Biochemical processes cause characteristic cell changes e.g. cell blebbing, shrinkage, DNA fragmentation and death. Tens of billions of cells undergo programmed death each day in the average human adult. Maintaining the homeostatic balance between cell proliferation and death is imperative for healthy functioning of an organism. Cell suicide is essential during embryonic development for tissue formation and finger separation, or when malfunctions emerge from cell stress or damage. Interest and research in apoptosis rose after discovery of its key role in many diseases. Insufficient apoptotic activity leads toward uncontrolled cell growth (tumour) and cancer, whereas excessive activity cause atrophy and neurodegenerative disorders such as Parkinson's, Alzheimer's and Huntington's diseases. The same apoptotic biochemical reactions can be seen in striated muscle cell after *Trichinella spiralis* infection.

The nematode *Trichinella spiralis* is an intracellular parasite of mammalian skeletal muscle cells. The parasite infects many species including rats and other rodents, pigs, bears and humans. *Trichinella* occupies the host cell without destroying it and can survive within it for a long period (up to several years) and infect other mammal hosts after its former host's death. After infested undercooked meat is eaten, adult worms mate. Larvae cross small intestine wall into blood stream and move to striated muscles and invade individual cells. Each worm start remodelling of the cell, which results in capsule composed of collagenous wall (parasite protection) and cellular components (called nurse cell) that nourish the parasite. Both parts, the wall and the nurse cell, are of host origin.

The main objective of this master thesis is to make algebraic interpretation of

apoptotic processes in muscle cells infected by *Trichinella spiralis*. The exact answers to question how is *Trichinella* accommodated by the muscle cell without killing the cell remain to be found. We will approach this problem from different angles and develop a mathematical model of apoptosis without and with influence of the parasite.

1 Apoptosis

Apoptosis can be initiated by a number of factors, including cell stress, cell damage, conflicting intra- or extracellular signals, genetic damage, drugs or radiation. Apoptosis activation can primarily be divided into two major pathways: extrinsic pathway, which is activated via death receptor signalling such as Fas (CD95) or tumour necrosis factor receptor (TNF-R). Mitochondria dependent intrinsic pathway is activated by cytochrome c release from mitochondria after stress or inflammation.

Binding of death ligands e.g. FasL or TNF concludes in oligomerization of the associated death receptors (TNF-R, Fas), followed by recruitment of adaptor protein - Fas associated death domain (FADD). Fadd serves as a bridge between the death receptors and procaspases-8. All of them together compose the death-inducing signalling complex (DISC).

As effect of DISC formation, procaspase-8 is cleaved resulting in formation of active caspase-8 initiating the apoptotic cascade reaction. Here two distinctive types of cell are known. Type I cells are characterized by activation of caspase-8 in immense quantities and following mitochondria independent activation of caspase-3 leading to cell death. In contrast, type II cells generate small number of active caspase-8 and cascade needs to be amplified by mitochondria.

Amplification occurs by cleaving of Bid by caspase-8 to trincated Bid (tBid) and consecutive transfer into mitochondria and reacting with Bax, which promotes release of proapoptotic molecules like cytochrome c and smac/DIABLO to cell's cytoplasm. This process is inhibited by Bcl-2 reacting with Bax and forming an inactive compound. Several cytochromes c and Apoptotic protease activating factors-1 (Apaf-1) are needed to form apoptosome complex by binding to each other and prompt activation of procaspase-9 to caspase-9, which in succession converts procaspase-3 to its active

form caspase-3. This serves as the beginning of proapoptotic loop i.e. intense caspase-8 activation and Bcl-2 inactivation. The inhibitors of apoptosis (IAP) suppress programmed cell death by joining with both caspase-3 and caspase-9.

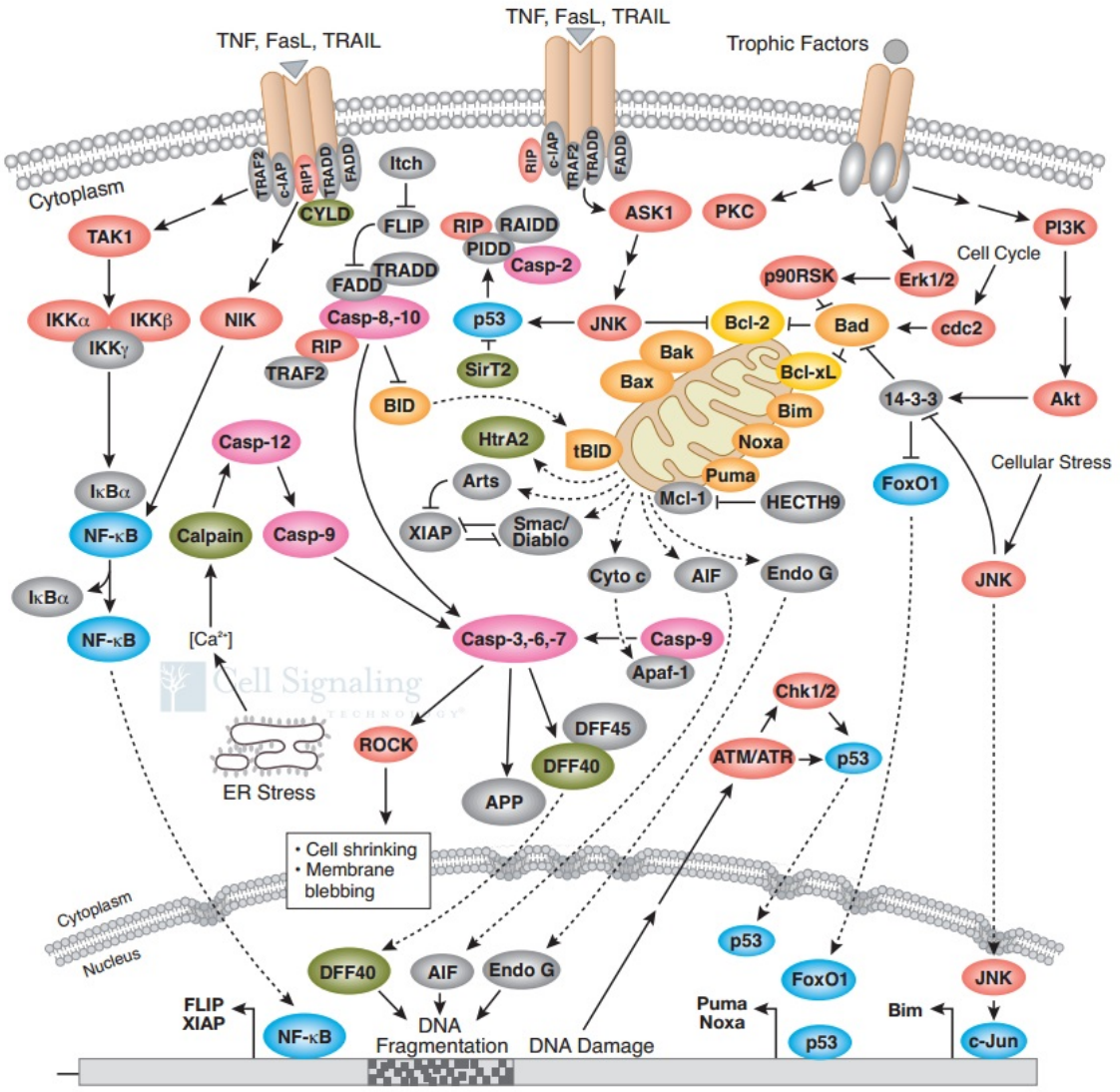

Figure 1: Regulation of Apoptosis Signaling Pathway[1]

The importance of researching the apoptosis rose significantly in recent decades. According to Cancer.org (2008) malignant neoplasm is the second leading cause of death worldwide with more than 7.4 million deaths. The perspective for future is not bright and number of people affected by tumours will only rise. Fussenegger et al. (2000) showed that cancerous cells do not delay or have no reaction to apoptotic

[1] http://www.cellsignal.com/contents/science-cst-pathways-apoptosis/regulation-of-apoptosis-signaling-pathway/pathways-apoptosis-regulation

signals . Malfunctioning cells divide, but do not die. This is the reason, why tumors grow.

As we can see on Fig. 1, the described reactions are just a glimpse of all the complex relations between substances inside of a cell during apoptosis. Research of complex biochemical system takes time and resources. Mathematical modelling can help in this matter, so that less laboratory tests are needed to be done. With today's accessibility of computers it is easier and cheaper to simulate responses and behaviour of known reactions in a cell to a drug, than to make numerous laboratory tests.

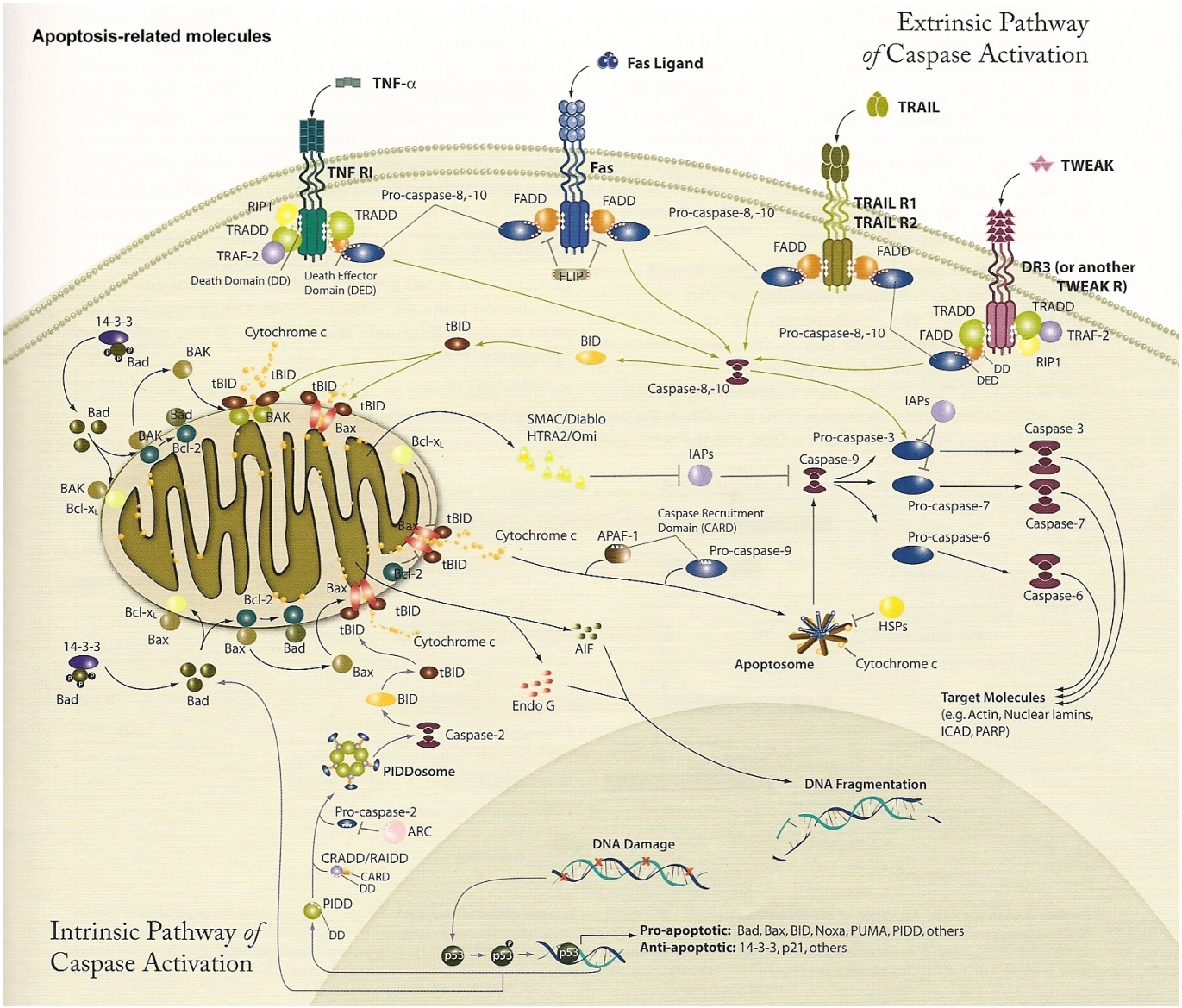

Figure 2: Apoptosis regulated molecules [2]

[2] http://www.hixonparvo.info/apoptosis.jpg

2 Trichinella spiralis

2.1 Secretions

When *Trichinella spiralis* passes through intestinal epithelial cells, these cells do not display visible damage. Observations of areas occupied by worms revealed only sporadic caspase-3 activation and increased concentrations of AIF and Bax. Slight change of Bcl-2 distribution inside the cell was detected. No significant changes of expression of proteins associated with apoptosis were spotted in the cells surrounding the worms.

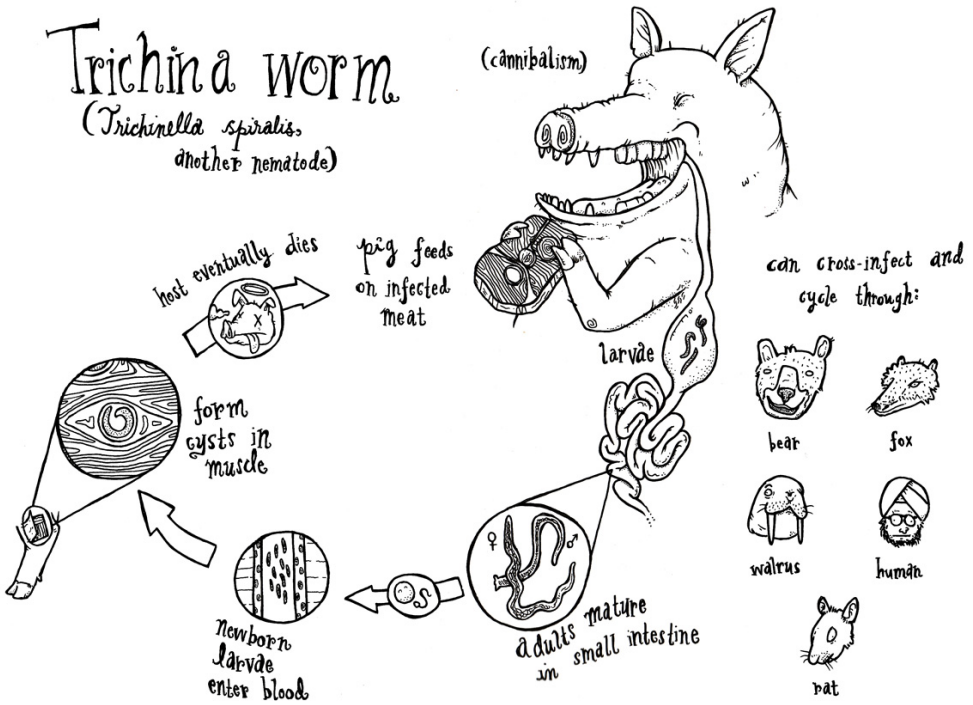

Figure 3: Life cycle of *Trichinella spiralis* worm[3]

[3]https://archive.org/details/Lifecycles

It is interesting, that the presence of *Trichinella* does not influence intestinal cells the same way as striated muscle cells (P. Babal, personal communication, August, 2013).

According to Milcheva et al. (2013) *Trichinella* stimulates sialyltransferase activity in striated muscle cells and causes an increase of free sialic acid levels in cells. Intense distribution of sialylated glycoconjugates a (certain carbohydrate class) in infected fibres was found, while they are absent in healthy fibres. These worms, however do not synthesize sialic acids. Elevated levels of sialic acids and sialylation of glycoproteins affect many cell functions and can be advantageous to parasite accommodation.

In addition to this, *Trichinella* worms release variety of proteins, which are likely to guide muscle cell transformation and capsule formation. Excreted proteins change during a lifespan of the worm and are specific only to certain periods of parasite's life (Nagano et al., 2009).

Despommier (1998) stated, that *Trichinella* secretes signalling molecules (cytokines), which coordinate behaviour of cell. Response to those signals is arrest in G2/M phase of cell cycle, synthesis of collagen capsule, angiogenesis (forming of new blood vessels), mitochondrial damage. Furthermore, worm does not rest inside of the cell. It constantly moves inside.

2.2 Rejected features of the model

From all this information, we tried to find the best possible way, how can Trichinella direct processes and disrupt the process of apoptosis inside the cell in our model. In this section, we will explore few ideas, which in the end were abandoned.

2.2.1 Structure of striated muscle cell and communication with nucleus

From our personal communication with Babal (2013), we learned that muscle cells behave differently in comparison to other cells in a mammalian body, mainly the healing process after injury of the cell. Laboratory observations showed, that there is a resemblance between activities or nurse cell formation and regeneration of skeletal

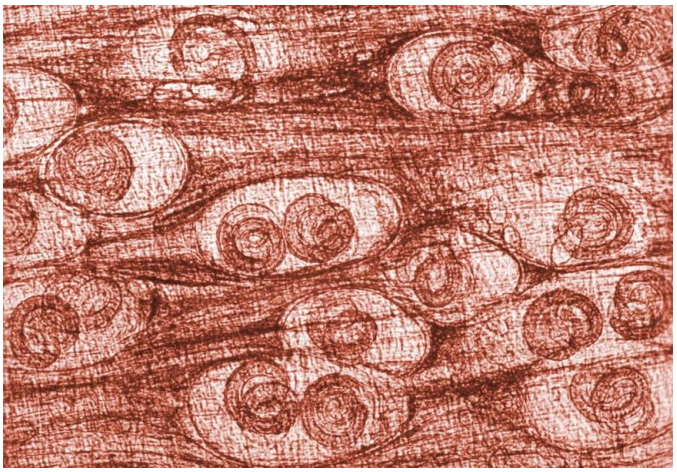

Figure 4: Cysts of *Trichinella spiralis* worms within muscle tissue[4]

muscle cell after injury. Process of regeneration consists of four stages i.e.

- Activation of satellite cells
- Proliferation of satellite cells
- Differentiation and fusion
- Self-renewal of satellite cell

Injury causes inflammation and activation of mononucleated cells. After macrophages clean cellular debris, so it will not spread into surrounding area, which could result in more harm. Satellite cells are activated, they proliferate and fuse with damaged fibres. During this period, previous muscle cell nucleus is replaced by a new one from satellite cells and this activity continues until muscle fibre is completely healed.

Following the invasion of Trichinella into the cell, a similar response in the affected area can be seen (Wu et al., 2008). After a nucleus disappears, newly formed nuclei surround the worm and do not spread in the fibre.

Start of the healing process in the muscle cell is in opposition to the passing of the worms through intestinal wall.

As we lacked the key information about the substances that direct actions inside of a cell occupied by Trichinella, we did not include this feature to our model of apoptosis.

[4]http://publichealth.lacounty.gov/acd/Diseases/Trichinosis.htm

2.2.2 Connection of Ca^{2+}, endoplasmic reticulum, mitochondrion, and AIF

Orrenius et al., (2003) examined the influence of changes in a Ca^{2+} concentration changes inside a cell. Small alterations in the amount of Ca^{2+} could help with signalling within the cell. Spasmodic influx of Ca^{2+}, however, can serve as proapoptotic stimuli. Elevated quantity of Ca^{2+} were found in cells affected by ischemia (blood supply restriction to tissue). This fact also concurs with angiogenesis and it is only logical that a parasite wants to be fed.

Sorting of newly synthesized proteins, Ca^{2+} storage, and signalling are one of the main functions of Endoplasmic reticulum (ER). Any disruption in these processes can lead to ER stress. Prolonged stress stimulates the release of Ca^{2+} from pool or cleavage of procaspase-12 that consecutively activates procaspase-3 and procaspase-9.

Mitochondria are known to actively participate in Ca^{2+} concentration changes. Uptake of Ca^{2+} is under normal conditions subtle and serves mostly as part of mitochondrial energy dissipating cycle. Pathological conditions in a cell can cause accumulation of Ca^{2+} and subsequently overload. That poses as oxidative stress and trigger permeabilization of mitochondrial membrane and promotes the release of cytochrome c, $smac/DIABLO$, and most importantly AIF particles.

We ruled Ca^{2+} signalling out because we learned from our personal communication with Babal (2013) that the amount of burst AIF release does not agree with the quantity stored and synthesized in mitochondria. He also did not make laboratory observations of Ca^{2+} concentration.

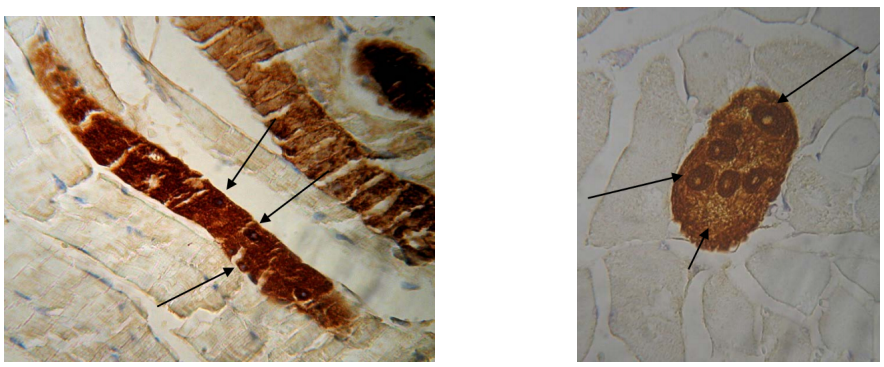

Figure 5: AIF accumulation in cell (brown) 10 and 14 days post-infection (Babal, P., 2011)

2.3 Influence of Trichinella in our models

Despommier (1998) detected mitochondrial damage i.e. vacuolization of inner mitochondrial matrix only five days after the worm invaded the muscle cell. Furthermore, Wu et al. (2008) observed changes in a cytoplasm of a cell, increased amount of endoplasmic reticulum and disappearance of swelled mitochondria that were replace by new and smaller mitochondria with hyper-density matrix. This information also agrees with the possible effect of high Ca^{2+} concentration inside infected cell.

We, therefore, decided to incorporate disappearance of mitochondria after set time into our two models without searching for the exact cause. We introduce new variable *mit* that until the certain time will have value 1 and then gradually decreases exponentially until it reaches 0. All the compounds that are produced or stored in mitochondria will be affected through their production rates Ω and concentrations stored inside by the degradation rate of mitochondria.

Take cytochrome c_{mito} for example which under normal condition would be defined by ODE (15)

$$\frac{c_{mito}}{dt} = \dot{[c_{mito}]} = \Omega_{c_{mito}} - \mu[c_{mito}] - k_3[Bax_2][c_{mito}]$$

After we put in the disappearance of mitochondria:

$$\frac{c_{mito}}{dt} = \dot{[c_{mito}]} = mit\Omega_{c_{mito}} - \mu[c_{mito}] - k_3[Bax_2][c_{mito}] + \frac{dmit}{dt}[c_{mito}]$$

where

$$\frac{dmit}{dt} = \dot{mit} = r_{mito} * mit$$

To keep the number of mitochondria unchanged during the initiation phase of reactions when parasite has no effect on them, we will assign $rmito = 0$ for this period and small negative value in the range $< -10^{-3}, -10^{-5} >$. Finally, we will slowly turn the mitochondria on again by assigning positive value in the range $< -10^{-5}, -10^{-3} >$ to *rmito*. What would we like to see by turning off the mitochondria is slow down of apoptosis that will not start again with newly form mitochondria.

Variables affected by the function $mit(t)$: Bax, Bax_2, and c_{mito} in reduced model. Bax, Bax_2, c_{mito}, Aif_{mito}, $Smac_{mito}$, and *Bcl*-2 in the whole model.

3 Reduced Mathematical Model of Apoptosis

At first, we will look at the reduced mathematical model. Our proposed full model of apoptosis consists of 43 variables with one ordinary differential equation for each variable. In addition to that, we need to use a considerable number of reaction rate constants k_x and other parameters as synthesis constants Ω_x and degradation constant μ. Unfortunately these parameters are not know in general so we will use values within the range of previously adopted parameters by Bagci et al. (2006) and Chen et al. (2000)

Therefore, we propose reduced model of apoptosis composed of 12 variables: procaspase-8 ($PC8$), caspase-8 ($C8$), Bid, $tBid$, Bax, Bax_2, cytochrome c_{mito} and c, $Apaf$-1, procaspase-3 ($PC3$), caspase-3 ($C3$) and IAP with two amplification feedback loops and partially compare our results with results obtained from other simplified models proposed by Bagci et al. (2006).

3.1 Quest for a bistable system

Nair et al. (2004) noticed bifurcation into two states preferring either cell death or survival from observations of cells under oxidative stress. Each cell activates homeostatic or apoptosis signals in a matter of minutes after hydrogen peroxide (H_2O_2) exposure. The bistable behaviour between these two opposing responses is proposed to be a stochastic process (Nair et al., 2004).

Study made by Bentele et al. (2004) points attention to transition from cell survival to cell death after certain stimuli exceeded threshold values. These information give

us insight that bistability is a functional attribute in cellular systems and thus we will also search for bistable behaviour in a similar way as Bagci et al. (2006).

Activation of caspase-8

Maintained caspase-8 activation should have served as the initial impulse for the system. Nevertheless, it leads to system where no bistability was present in all simulations we ran independently with different ranges of other parameters. We managed to achieve bistability only when rate constant of self-activation, instead of activation by DISC, was equal to zero. As we look for bifurcation into two states in our system we leave the cleavage of procaspase-8 solely on caspase-3 feedback loop.

Self-activation leads to a monostable system favouring only cell death because no specific stimuli is needed to start apoptosis cascade reactions i.e. accumulation of active caspase-8 could be the trigger. We previously thought that we can omit inhibitory molecule BAR and set the rate to lower levels, which was not true. Assigning positive value to the parameter only for a brief period did not work neither.

$$PC8 \xrightarrow{k_k} C8 \qquad k_k = 0\mu M^{-1}s^{-1} \quad (1)$$

Cleavage of Bid by caspase-8

We omitted creation of $C8 \cdot tBid$ compound.

$$C8 + Bid \xrightarrow{k_1} C8 + tBid \qquad k_1 = 10\mu M^{-1}s^{-1} \quad (2)$$

Release of cyt c from mitochondria to cytoplasm

We propose much straightforward Bax_2 channel formation and cytochrome c release, compared to the full model where this process is defined by 4 equations. Every reaction occurs in close proximity to outer mitochondrial membrane i.e. excluding $tBid$ translocation into mitochondria.

$$tBid + 2Bax \xrightarrow{k_2} tBid + Bax_2 \qquad k_2 = 10\mu M^{-1}s^{-1} \quad (3)$$

$$Bax_2 + cyt\ c_{mito} \xrightarrow{k_3} Bax_2 + cyt\ c \qquad k_3 = 10\mu M^{-1}s^{-1} \quad (4)$$

Activation of caspase-3

We retain cooperativity of seven cytochromes c and $Apaf$-1 molecules. On the other hand, we leave out apoptosome formation and tricky activation of caspase-9. We acquire one simple reaction with one reaction rate constant instead of 11 reactions and 19 reaction rates. Excluding so much information can have uncertain consequences, but making the reduced model of apoptosis would not be possible without it.

$$7cyt\ c + 7Apaf\text{-}1 + PC3 \xrightarrow{k_6} 7cyt\ c + 7Apaf\text{-}1 + C3 \qquad k_6 = 10\mu M^{-14}s^{-1} \quad (5)$$

Loop cleavage of Bid by caspase-3

First feedback loop of reduced apoptosis model.

$$C3 + Bid \xrightarrow{k_8} C3 + tBid \qquad k_8 = 10\mu M^{-1}s^{-1} \quad (6)$$

Loop activation of caspase-8 by caspase-3

Second feedback loop of reduced apoptosis model.

$$C3 + PC8 \xrightarrow{k_a} C3 + C8 \qquad k_a = 10\mu M^{-1}s^{-1} \quad (7)$$

Inhibition of caspase-3 by IAP

Here IAP inhibits active caspase-3, but IAP itself stays active. The difference can be reduced by lowering production rate of IAP or raising its decomposition rate μ

$$C3 + IAP \xrightarrow{k_x} C3_{inactive} + IAP \qquad k_x = 1\mu M^{-1}s^{-1} \quad (8)$$

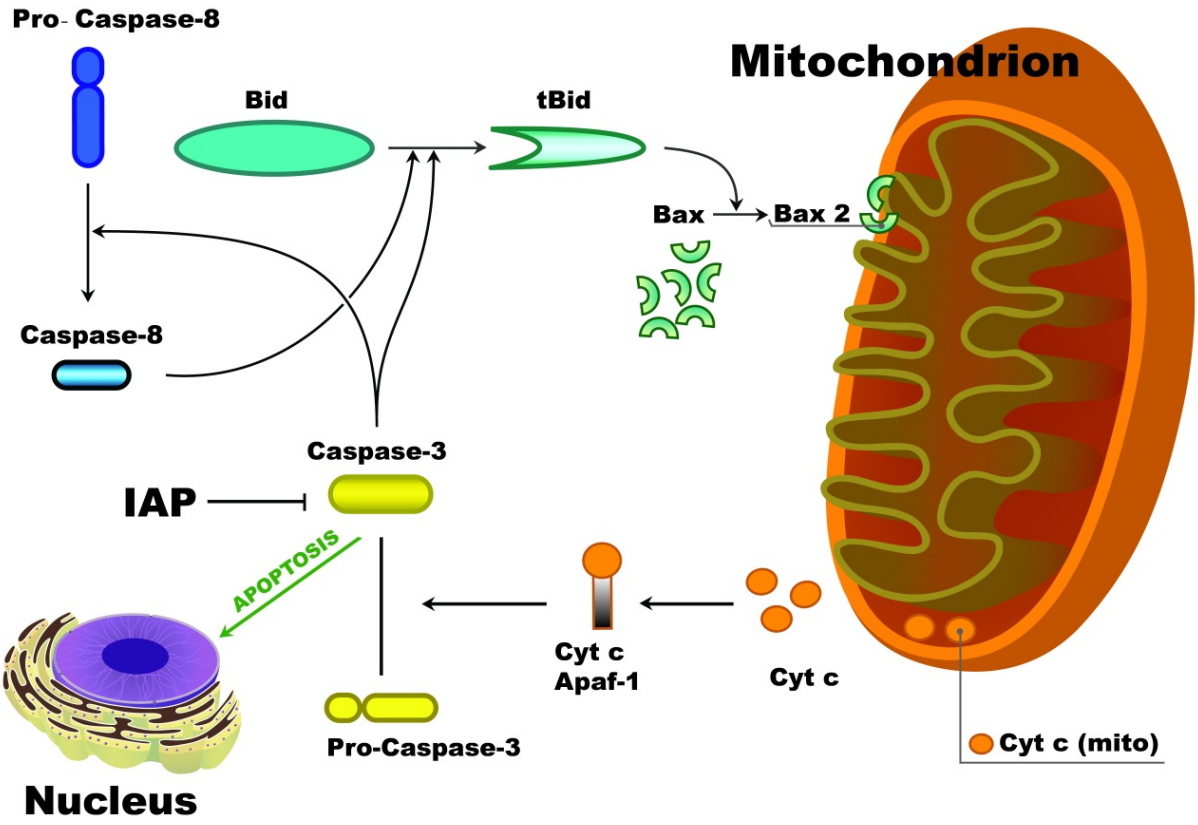

Figure 6: Graphic presentation of the reduced model equations and relations[5]

[5]Illustrated by Wang, Q. (2014)

3.2 Ordinary differential equations (ODE)

3.2.1 Short example of making ODE from biochemical reaction

Let's say we have a biochemical system where substrate-1 ($S1$) and substrate-2 ($S2$) bind together with rate k to form a compound (C) defined by the flux J:

$$S1 + S2 \xrightarrow{k} C \qquad k = 10\mu M^{-1}s^{-1} \qquad J$$

When we want to analyse the system, we have to translate the reaction into a set of ordinary differential equations. We thus introduce flux J that simplifies expressions considerably, especially for greater and more complicated systems.

$$J = k[S1][S2]$$

Using the flux J we can write the ODE:

$$[\dot{S1}] = \Omega_{S1} - \mu[S1] - J$$
$$[\dot{S2}] = \Omega_{S2} - \mu[S2] - J$$
$$[\dot{C}] = -\mu[C] + J$$

Concentrations of substances are written as [S1], [S2], and [C]. Amount of substrates in the system is maintained by inflow or synthesis which is described by Ω_{S1} and Ω_{S2}. All compounds have certain degradation rate defined by μ. Both substrates are used in the process of forming the compound with the rate k i.e. decrease of concentrations of substances and increase of compound concentration by $J = k[S1][S2]$.

3.2.2 ODE of the reduced model

Biochemical reactions are translated into system of ordinary differential equations, where Ω_X is production rate of molecule X and μ decomposition rate of substance. The reduced model is easy enough so we will not use the flux form until the whole mathematical model of apoptosis.

The kinetic reaction rates are defined above with related reactions (1)-(8). We set degradation rate $\mu = 0.004$ and conduct parametric study based on adjusting the Ω parameters.

Here are the differential equations of the reduced system:

$$\dot{[PC8]} = \Omega_{PC8} - \mu[PC8] - k_k[PC8] - k_a[PC8][C3] \tag{9}$$

$$\dot{[C8]} = -\mu[C8] + k_k[PC8] + k_a[PC8][C3] \tag{10}$$

$$\dot{[Bid]} = \Omega_{Bid} - \mu[Bid] - k_1[C8][Bid] - k_8[C3][Bid] \tag{11}$$

$$\dot{[tBid]} = -\mu[tBid] + k_1[C8][Bid] + k_8[C3][Bid] \tag{12}$$

$$\dot{[Bax]} = mit\Omega_{Bax} - \mu[Bax] - 2k_2[tBid][Bax]^2 + r_{mito}mit[Bax] \tag{13}$$

$$\dot{[Bax_2]} = -\mu[Bax_2] + k_2[tBid][Bax]^2 + r_{mito}mit[Bax_2] \tag{14}$$

$$\dot{[c_{mito}]} = mit\Omega_{c_{mito}} - \mu[c_{mito}] - k_3[Bax_2][c_{mito}] + r_{mito}mit[c_{mito}] \tag{15}$$

$$\dot{[c]} = -\mu[c] + k_3[Bax_2][c_{mito}] \tag{16}$$

$$\dot{[Apaf\text{-}1]} = \Omega_{Apaf\text{-}1} - \mu[Apaf\text{-}1] \tag{17}$$

$$\dot{[IAP]} = \Omega_{IAP} - \mu[IAP] \tag{18}$$

$$\dot{[PC3]} = \Omega_{PC3} - \mu[PC3] - k_6[c]^7[Apaf\text{-}1]^7[PC3] \tag{19}$$

$$\dot{[C3]} = -\mu[C3] + k_6[c]^7[Apaf\text{-}1]^7[PC3] - k_x[C3][IAP] \tag{20}$$

$$\dot{mit} = r_{mito} * mit \tag{21}$$

3.3 Steady state of the system and stability analysis

We ran simulations with multiple starting points in the twelve dimensional system with fixed parameters during each simulation and observed the dynamics. Subsequently we tried to justify the observed phenomena, so we searched for fixed points (equilibria) of the system.

Fixed points are obtained by setting condition $\frac{dX}{dt} = 0$ for every ODE i.e. concentrations of compounds remain unchanged in time despite the ongoing reactions that aim to change them. Following elimination of variables leads to cytochrome c polynomial of degree 16 whose solutions are the equilibria we are looking for. We can, however, rule out all negative solutions and solutions with notable imaginary part. From that, all concentrations of other substances can be derived.

For further observations we need to assess stability of the fixed points therefore, we construct Jacobian matrix whose each line corresponds to particular ODE of variable

and rows contain partial derivations of first degree e.g. equations

$$\dot{x} = x + 2y \qquad\qquad \dot{y} = 3x + 4y$$

have Jacobian matrix such as:

$$J = \begin{bmatrix} \frac{d\dot{x}}{dx} & \frac{d\dot{x}}{dy} \\ \frac{d\dot{y}}{dx} & \frac{d\dot{y}}{dy} \end{bmatrix} = \begin{bmatrix} 1 & 2 \\ 3 & 4 \end{bmatrix}.$$

After that we substitute computed values of fixed points for designated variables still present in Jacobian matrix and find its eigenvalues. We interest ourselves in eigenvalues for apply:

- If the eigenvalues are all negative it is a stable node
- All positive eigenvalues mean unstable node
- Stable spiral in those dimensions where eigenvalues $\lambda_{\pm} = -\alpha \pm i\beta$ where $\alpha, \beta > 0$
- Unstable spiral in those dimensions where eigenvalues $\lambda_{\pm} = \alpha \pm i\beta$ where $\alpha, \beta > 0$

This master thesis is not the right place to try to discover all possible combinations of eigenvalues for 12 dimensional system but generally if eigenvalue is negative the fixed point is stable in that dimension and vice versa for positive eigenvalue.

In our search for bifurcation that indicates a bistable system, we will set $r_{mito} = 0$. Otherwise we would from (21) get a stable system where $mit = 0$. Thus, we will look for the bifurcation in our model by changing the values of all Ω normally influenced by mit and completely leave out the 13th differential equation that describes changes of the variable mit.

All the solutions can be gained from cytochrome c polynomial:

$$\begin{aligned} 0 =& K^2 R_{L0} + [c](-2KJR_{L0} - M\Omega_{c_{mito}} R_{P0}) + [c]^2(J^2 R_{L0} + \mu M R_{P0}) + [c]^7(K^2 R_{L7}) \\ &+ [c]^8(-2KJR_{L7} - M\Omega_{c_{mito}} R_{P7}) + [c]^9(J^2 R_{L7} + \mu M R_{P7}) + [c]^{14}(K^2 R_{L14}) \\ &+ [c]^{15}(-2KJR_{L14} - M\Omega_{c_{mito}} R_{P14}) + [c]^{16}(J^2 R_{L14} + \mu M R_{P14}) \end{aligned}$$

where these substitutions were made to simplify the equation:

$$R_{L0} = \mu^2 P_{L0} + \mu\Omega_{PC3} P_{L1} + P_2 \Omega_{PC3}^2 \qquad R_{P0} = \mu^2 P_{P0} + \mu\Omega_{PC3} P_{P1} + P_2 \Omega_{PC3}^2$$

$$R_{L7} = 2\mu k_6 P_{L0} i^7 + k_6 \Omega_{PC3} P_{L1} i^7 \qquad R_{P7} = 2\mu k_6 P_{P0} i^7 + k_6 \Omega_{PC3} P_{P1} i^7$$

$$R_{L14} = k_6^2 P_{L0} i^{14} \qquad R_{P14} = k_6^2 P_{P0} i^{14}$$

$$P_{L0} = k_k O^2 L + k_8 k_a \Omega_{PC3}^2 + \Omega_{PC3} O N_1 \qquad P_{P0} = O^2 N_3 + k_8 k_a \Omega_{PC3}^2 + \Omega_{PC3} O N_2$$

$$P_{L1} = -2\mu k_8 k_a \Omega_{PC3} - \mu O N_1 \qquad P_{P1} = -2\mu k_8 k_a \Omega_{PC3} - \mu O N_2$$

$$P_2 = \mu^2 k_8 k_a$$

$$O = \mu + k_x x$$

$$N_1 = k_8 mi + k_a L \qquad N_2 = k_8 mi + k_a L + \mu k_a$$

$$N_3 = \mu mi + k_k L \qquad mi = \mu + k_k$$

$$L = k_1 \frac{\Omega_{PC8}}{\mu}$$

$$M = \frac{k_3 \mu^4}{k_2 \Omega_{Bid}} \qquad K = k_3 \Omega_{Bax} \Omega_{c_{mito}} \frac{1}{\mu}$$

$$J = k_3 \Omega_{Bax} + 2\mu^2$$

Parameters used in the reduced model:

$$\Omega_{PC8} = 6 * 10^{-4} \mu M s^{-1} \qquad \Omega_{PC3} = 6 * 10^{-4} \mu M s^{-1}$$

$$\Omega_{IAP} = 10^{-5} \mu M s^{-1} \qquad \Omega_{Bid} = 6 * 10^{-5} \mu M s^{-1}$$

$$\Omega_{Apaf\text{-}1} = 6 * 10^{-4} \mu M s^{-1} \qquad \mu = 0.004$$

$$\Omega_{c_{mito}} \in < 10^{-5}, 3 * 10^{-3} > \mu M s^{-1} \qquad \Omega_{Bax} \in < 10^{-5}, 3 * 10^{-3} > \mu M s^{-1}$$

Derived variables from the set of equations (9)-(20):

$$[Apaf\text{-}1] = i = \frac{\Omega_{Apaf\text{-}1}}{\mu} \qquad [IAP] = x = \frac{\Omega_{IAP}}{\mu}$$

$$[c_{mito}] = \frac{\Omega_{c_{mito}}}{\mu} - [c] \qquad [PC3] = \frac{\Omega_{PC3}}{\mu + k_6 i^7 [c]^7}$$

$$[Bax_2] = \frac{\Omega_{c_{mito}} - \mu[c_{mito}]}{k_3 [c_{mito}]} \qquad [c_{mito}] \neq 0 \quad i.e. \quad [c] \neq \frac{\Omega_{c_{mito}}}{\mu}$$

$$[Bax] = \frac{\Omega_{Bax}}{\mu} - 2[Bax_2] \qquad [C3] = \frac{\Omega_{PC3} - \mu[PC3]}{\mu + k_x x}$$

$$[PC8] = \frac{\Omega_{PC8}}{\mu + k_a [C3] + k_k} \qquad [C8] = \frac{\Omega_{PC8}}{\mu} \frac{k_a [C3] + k_k}{\mu + k_a [C3] + k_k}$$

$$[Bid] = \frac{\Omega_{Bid}}{\mu + k_8 [C3] + k_1 [C8]} \qquad [tBid] = \frac{\Omega_{Bid}}{\mu} - [Bid]$$

The condition $[c_{mito}] \neq 0$ is unnatural especially because after all mitochondria are lost this variable will be equal 0 in steady state as no source and storage will be present inside the cell. Fortunately we use these formulas only for the analysis of the steady states. We will analyse this problem further in the last section Discussion and Conclusion.

As we shown at the beginning of this section (3.3), we construct Jacobian matrix from partial derivations of equations number (9)-(20). This particular matrix is sparse we will write it as a block matrix.

$$J = \left[\begin{array}{c|c|c|c|c|c} J_{11} & 0 & 0 & 0 & 0 & J_{16} \\ \hline J_{21} & J_{22} & 0 & 0 & 0 & J_{26} \\ \hline 0 & J_{32} & J_{33} & 0 & 0 & 0 \\ \hline 0 & 0 & J_{43} & J_{44} & 0 & 0 \\ \hline 0 & 0 & 0 & 0 & J_{55} & 0 \\ \hline 0 & 0 & 0 & J_{64} & J_{65} & J_{66} \end{array}\right],$$

where individual blocks are:

$$J_{11} = \begin{bmatrix} -\mu - k_k - k_a[C3] & 0 \\ k_k + k_a[C3] & -\mu \end{bmatrix}, \qquad J_{16} = \begin{bmatrix} 0 & -k_a[PC8] \\ 0 & k_a[PC8] \end{bmatrix},$$

$$J_{21} = \begin{bmatrix} 0 & -k_1[Bid] \\ 0 & k_1[Bid] \end{bmatrix}, \quad J_{22} = \begin{bmatrix} -k_1[C8] - k_8[C3] - \mu & 0 \\ k_1[C8]k_8[C3] & -\mu \end{bmatrix}, \quad J_{26} = \begin{bmatrix} 0 & -k_8[Bid] \\ 0 & k_8[Bid] \end{bmatrix},$$

$$J_{32} = \begin{bmatrix} 0 & -2k_2[Bax]^2 \\ 0 & k_2[Bax]^2 \end{bmatrix}, \qquad J_{33} = \begin{bmatrix} -4k_2[tBid][Bax] - \mu & 0 \\ 2k_2[tBid][Bax] & -\mu \end{bmatrix},$$

$$J_{43} = \begin{bmatrix} 0 & -k_3[c_{mito}] \\ 0 & k_3[c_{mito}] \end{bmatrix}, \qquad J_{44} = \begin{bmatrix} -k_3[Bax_2] - \mu & 0 \\ k_3[Bax_2] & -\mu \end{bmatrix},$$

$$J_{55} = \begin{bmatrix} -\mu & 0 \\ 0 & -\mu \end{bmatrix}; \qquad J_{64} = \begin{bmatrix} 0 & -7k_6[PC3][Apaf\text{-}1]^7[c]^6 \\ 0 & 7k_6[PC3][Apaf\text{-}1]^7[c]^6 \end{bmatrix},$$

$$J_{65} = \begin{bmatrix} -7k_6[PC3][Apaf\text{-}1]^6[c]^7 & 0 \\ 7k_6[PC3][Apaf\text{-}1]^6[c]^7 & -k_x[C3] \end{bmatrix}, \quad J_{66} = \begin{bmatrix} -k_6[Apaf\text{-}1]^7[c]^7 - \mu & 0 \\ k_6[Apaf\text{-}1]^7[c]^7 & -\mu - k_x[IAP] \end{bmatrix}.$$

3.4 Results

With all the expressed variables, we write a programme in MATLAB® software that numerically solves the polynomial using the $roots(c)$ function and all derived variables. Numerical algorithms always produce errors, so we need to account for them with variable $eps = 10^{-5}$. Subsequently we omit all the negative values that are less than negative eps and assign NaN. Identically all complex solutions are left out in the same manner. Remaining outcomes are sorted and evaluated for stability and plotted with red and magenta for stable node and stable spiral, blue and cyan for unstable node and unstable spiral.

3.4.1 Change of the reaction rate

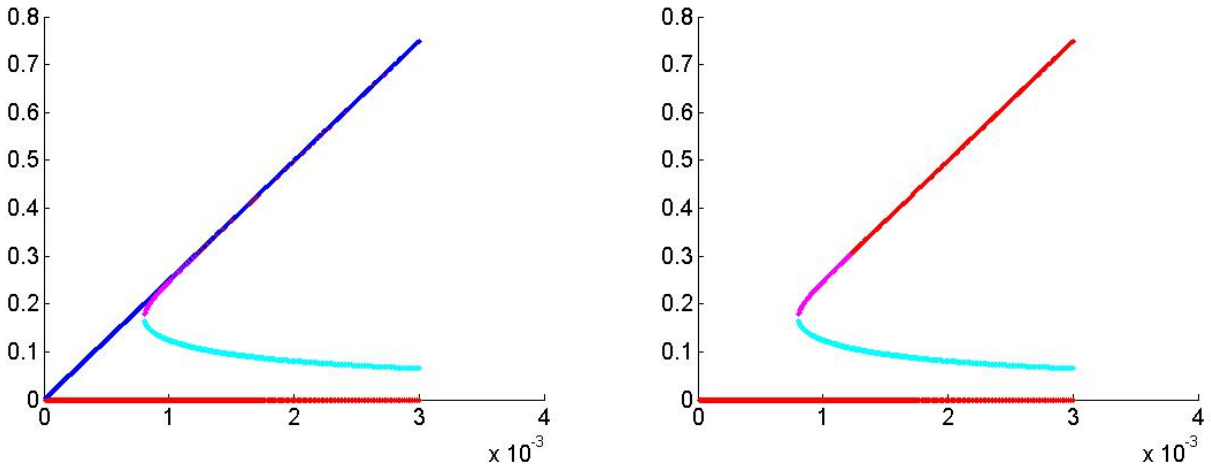

(a) With unstable blue line

(b) Without unstable blue line

Figure 7: Bifurcation and stability analysis of cytochrome c concentration in a cell. x-axis is Ω with units $[\mu M s^{-1}]$ and y-axis $[c]$ with units $[\mu M]$.

As it was hard to distinguish upper stable part of the bifurcation from unstable blue line on the picture (a), we made another without that part (picture (b)). Our first results look promising, we found stable nodes for cytochrome c concentration outside of mitochondria. Red line at the bottom with value next to 0 represents no apoptotic activity and the upper red line are stable nodes of $[c]$ during the process of cell death in respect to synthesis rate Ω of Bax, c_{mito}.

We chose value of Ω close to the point where bifurcation occurs for substances closely related to the mitochondria i.e. $\Omega_{c_{mito}} = 0.0008\mu Ms^{-1}$ and $\Omega_{Bax} = 0.0008\mu Ms^{-1}$ and observed time evolution of caspase-3 and caspase-8 (Fig. 8).

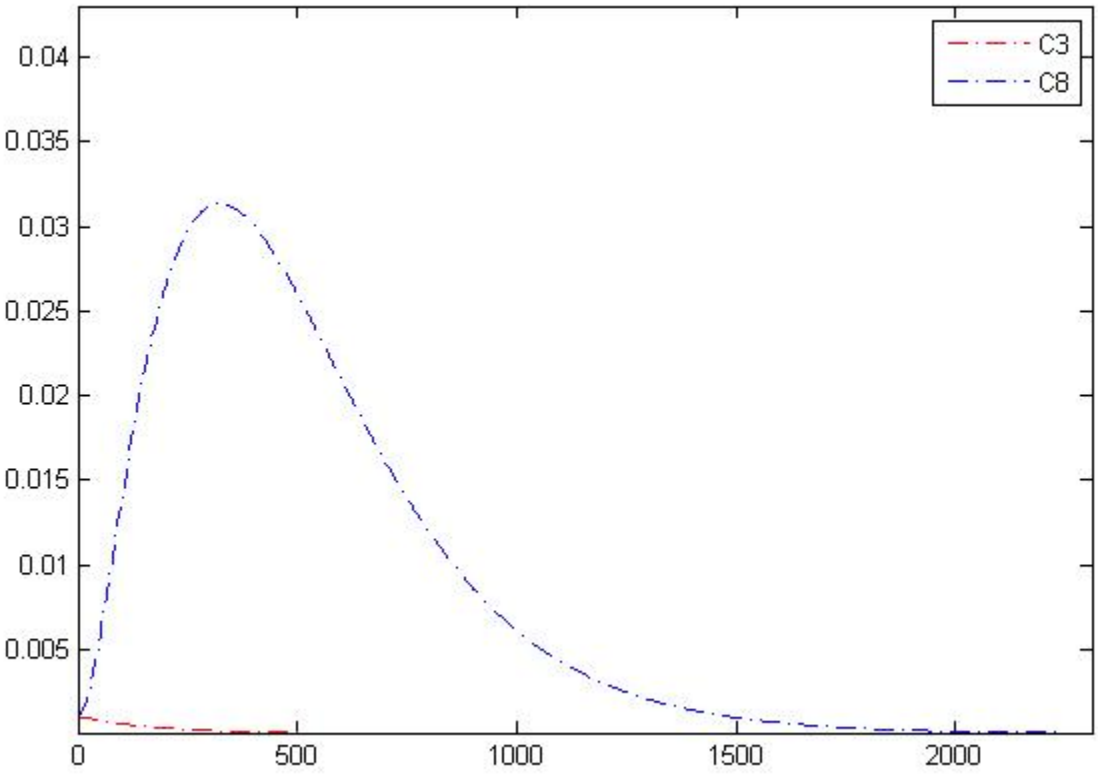

Figure 8: Time evolution of caspase-3 and caspase-8 in original reduced model of apoptosis ($[s]$ on horizontal axis and $[\mu M]$ on vertical axis).

In comparison to Bagci et al. (2006) the progress of the caspase-8 is in a similar range of concentrations. Amount of the active caspase-3 in cytoplasm is, however, very low. Thus, we compiled program for the whole model presented in the fourth chapter that is for some small adjustments almost identical to the model Bagci et al. (2006) ran simulations. The results were very different with higher activity of caspase-3 and roughly the same magnitude of concentration in the cytoplasm as caspase-8, so we turned our attention back to the model mainly where the biggest reduction occurred i.e. reaction (5).

Activation of procaspase-3 by cytochrome c and $Apaf$-1 left out 18 reactions. We investigated this phenomenon thoroughly, especially influence of the element with the

highest power: $k_6[c]^7[Apaf\text{-}1]^7[PC3]$. Here concentrations that are less than $1\mu M$ are both raised to the power of 7. Compared to the full model where binding of c and $Apaf$-1 is a simple process (reaction (31)) and cooperativity of that complex is in reaction (32) translated only to the power of 4 with reaction rate of apoptosome formation equal approximately to $500\mu M^{-3}s^{-1}$.

Therefore, after multiple simulations of reduced dynamic system we proposed change of the rate k_6 to $6 * 10^8 \mu M^{-14} s^{-1}$ which resulted in the Fig. 9.

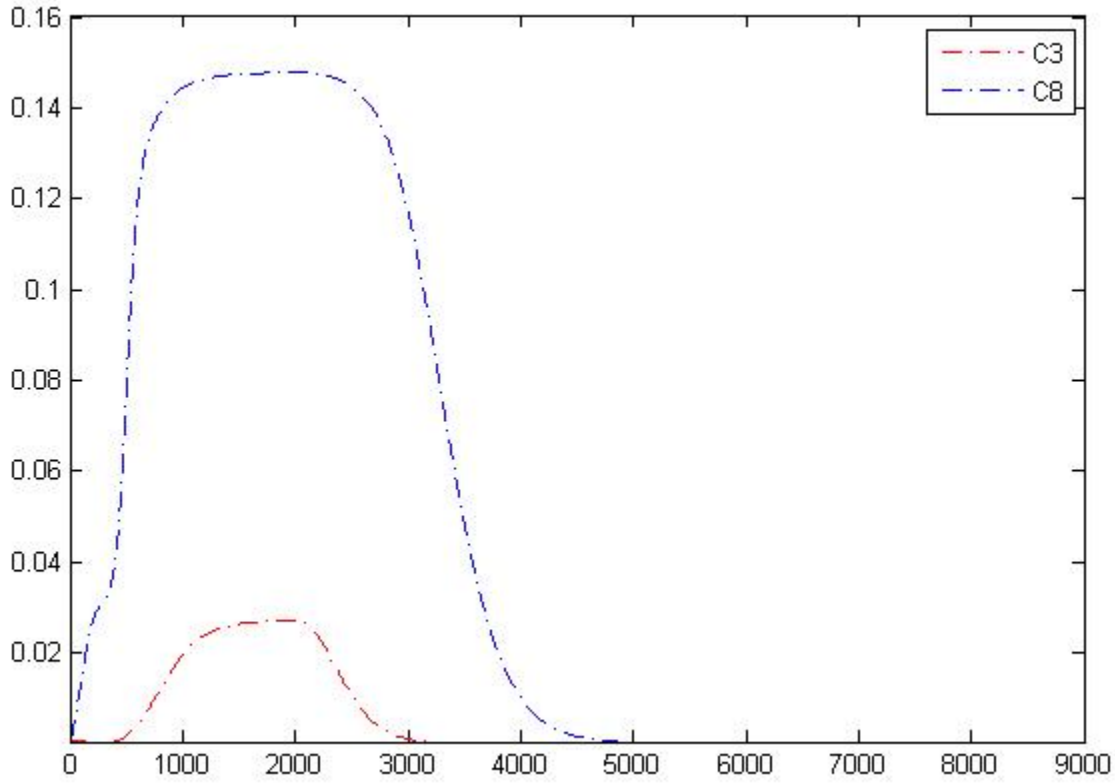

Figure 9: Time evolution of caspase-3 and caspase-8 in adjusted reduced model of apoptosis ($[s]$ on horizontal axis and $[\mu M]$ on vertical axis).

In both cases turning off the mitochondria takes place exactly at 2000 seconds. As we can see, the ratio of concentrations of caspase-3 and caspase-8 is large compared to the ratio $1:7$ in adjusted model. Furthermore, all active caspases deteriorated sooner than they could reach the set boundary of 2000 seconds when the mitochondria start to deteriorate by rate $r_{mito} = -0.001$.

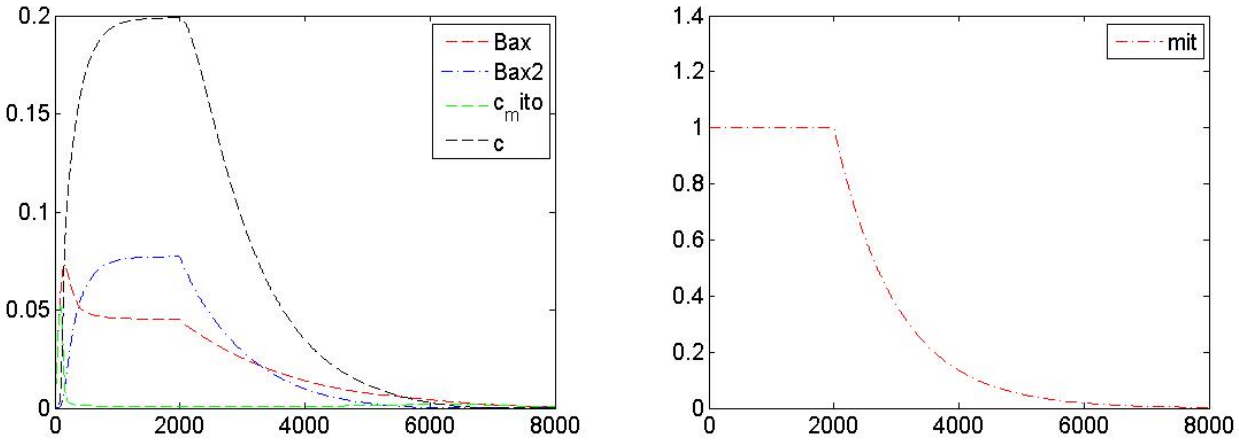

(a) Proteins associated with mitochondria

(b) Mitochondria decay

Figure 10: Time evolution of mitochondrial decay and related proteins Bax, Bax_2, c_{mito}, and c ($[s]$ on horizontal axis and $[\mu M]$ on vertical axis (a), ratio of active mitochondria (b)).

When we look at the dynamics of the system, it more or less copies the behaviour of its key part mitochondria. What we see is putting a halt to ongoing apoptosis by removal of the mitochondria, fade of all the substances stored or produced within mitochondria (Bax, Bax_2, and c_{mito}) and slow decay of all the other active substances by the rate μ. All other proteins such as $PC8$, Bid, $PC3$, IAP, and $Apaf$-1 will be produced continually until all of them reach their own steady state.

3.4.2 New Ω and spawn of mitochondria

Changing the reaction rate of caspase-3 activation surely had an impact on the stability and fixed points. We, therefore, alter our program for solving fixed points, input the new constant and assess the outcome seen on the Fig. 11.

The limit point of the bifurcation in the system moved from roughly $\Omega_{Bax} = \Omega_{c_{mito}} \approx 8 * 10^{-4} \mu M s^{-1}$ to $\Omega_{Bax} = \Omega_{c_{mito}} \approx 1.14 * 10^{-4} \mu M s^{-1}$. The value is now closer to the value obtained by Bagci et al. (2006), but then again they were evaluating the system by altering caspase-3 concentration simultaneously with Ω_{Bax} resulting in the limit point $\Omega_{Bax} \approx 6 * 10^{-6} \mu M s^{-1}$. This is, however, not the only change that occurred. The hyperbola asymptotically approaches the other solutions slowly, compared to the model with original reaction rate $k_6 = 10 \mu M^{-14} s^{-1}$.

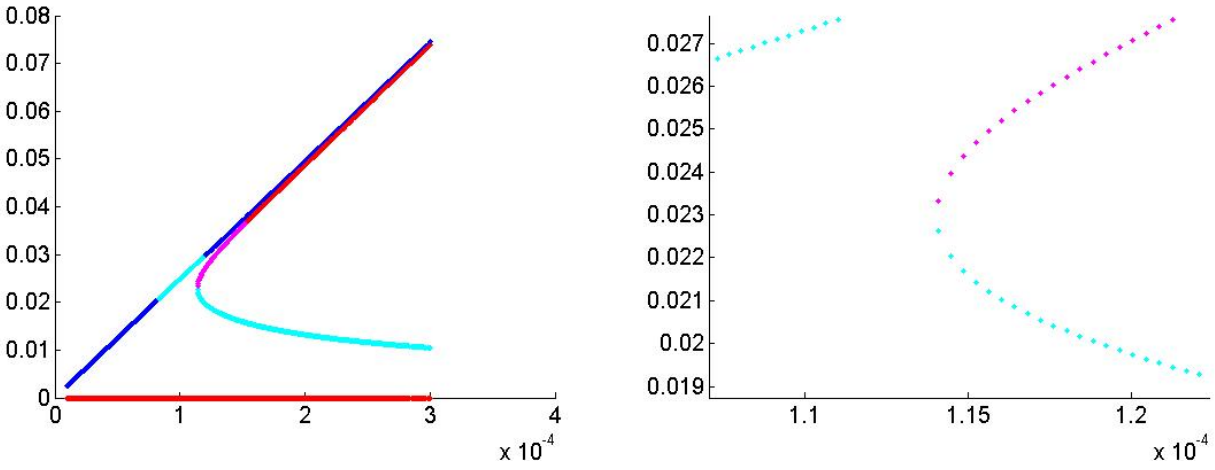

Figure 11: Whole and zoomed bifurcation diagram for $[c]$ (on horizontal axis is Ω with units $[\mu M s^{-1}]$ and on vertical is $[c]$ with units $[\mu M]$.

From research papers mentioned in chapter 2, we know that new smaller mitochondria appear in the cytoplasm of a cell after the original disappear but apoptosis does not start anymore. These newly formed organelles are smaller in size and thus can have altered functionality. In the previous experiment, we successfully stopped apoptosis by removing the mitochondria from the cell. Here we will wait for considerable depletion of all active substances and turn them back on analogically. After comparing the changes in dynamics of the system in respect to parameter r_{mito},

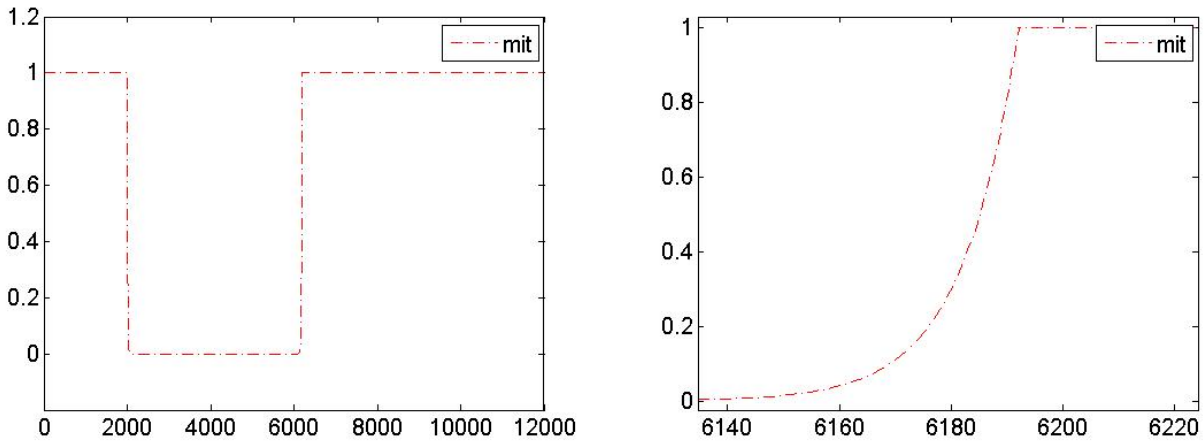

Figure 12: Time evolution of the mitochondria([s] on horizontal axis, ratio of working mitochondria on vertical axis).

we decided to deplete the mitochondria rapidly by setting $r_{mito} = -0.1$. By doing this, we achieve quicker computing time in exchange for swift changes toward the stable state and condensed graphs that can be seen below (Fig. 13).

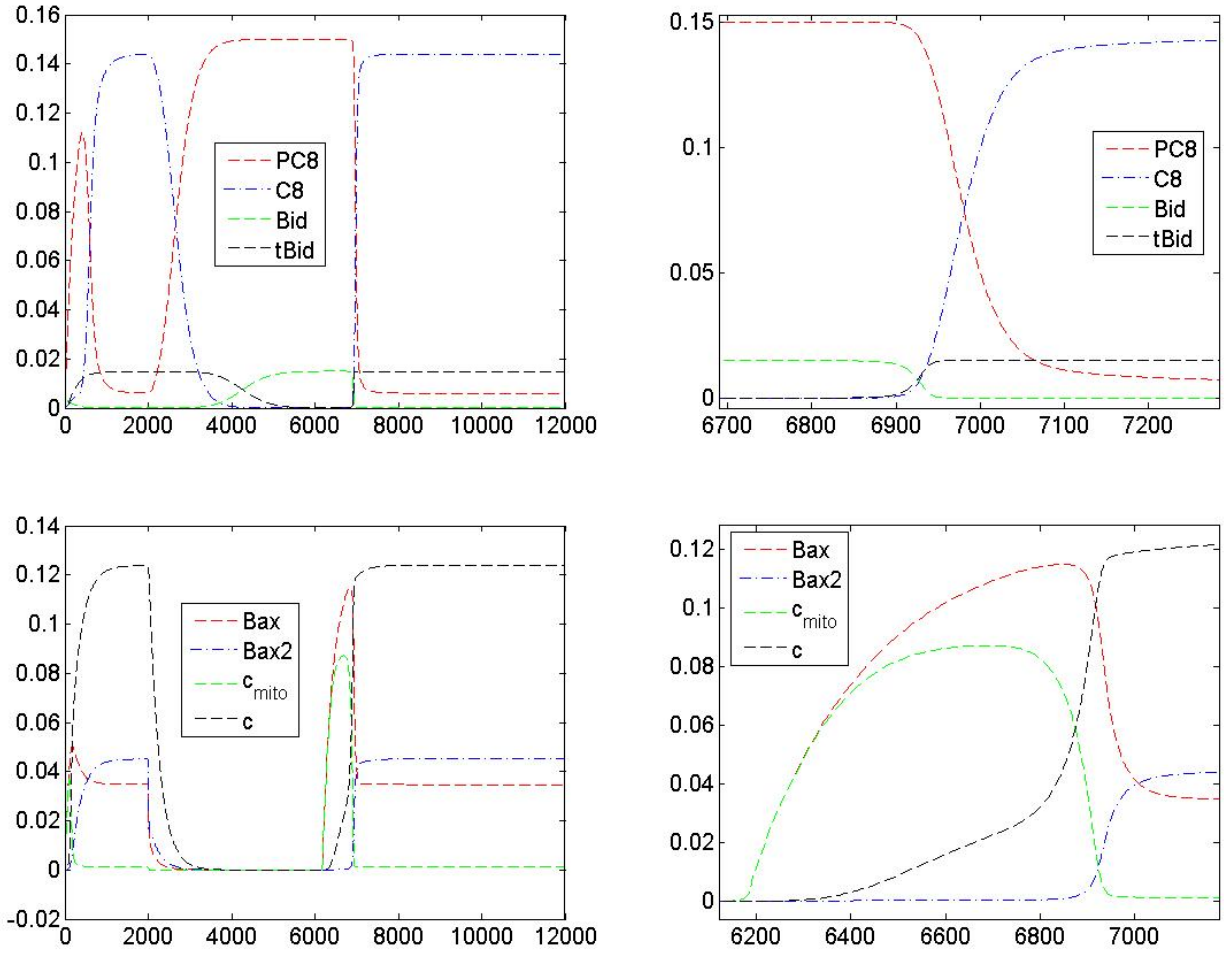

Figure 13: Time evolution of some proteins in full time frame on the left and zoomed into area of the start of newly formed mitochondria ($[s]$ on horizontal axis, $[\mu M]$ on vertical axis).

What the figures above are showing is starting of the programmed cell death in the first 2000 seconds. Substances with close relation to mitochondria are first to vanish from the system, but it takes much longer to exhaust all the caspase-8 and $tBid$. The next important time point is $T = 5500s$, when new mitochondria start to emerge exponentially. Almost 700 seconds pass until the system is saturated with these organelles. When we examine the lower left picture, we can see the rising concentration of Bax and c_{mito} within mitochondria, but with no Bax_2 which serves as a channel

to release cytochromes into cytoplasm. The fascinating phenomenon is leakage of c_{mito} (green line) even with Bax_2 concentration near zero and around time point 6900 seconds, we can see the start of the apoptosis (concentration of executioner caspase-3 at the same levels as in the time frame from 0 to 2000 seconds, data not shown).

Anther possible explanation is that system approaches unstable spiral as the mitochondria are forming i.e. production rate Ω of Bax and c_{mito} are rising to the value $\Omega = 5 * 10^{-4}$ (moving toward the cyan line on the left picture of Fig. 10) and later crossing to the big hyperbolic area. The system starts to move to the new stable fixed point (red line) i.e. apoptosis.

To account for numerical errors made by solver program, we ran separate simulations with starting point that contained high concentrations of $PC8$, Bid, $PC3$, IAP, and $Apaf\text{-}1$, low $C8$, $tBid$, c, and $C3$ concentrations that served as stimuli, and values of Bax, Bax_2, and c_{mito} equal to 0. The triggered apoptosis had similar dynamics to the one, we can observe on Fig. 13 from time point $t \approx 6190s$.

3.4.3 Small mitochondrion equals deficient mitochondrion

It is apparent that morphologically changed mitochondria can not function in the same way as original mitochondria do. We, therefore, analysed changes in the system in respect to the variable *mit* for the newly formed organelles. What we found was

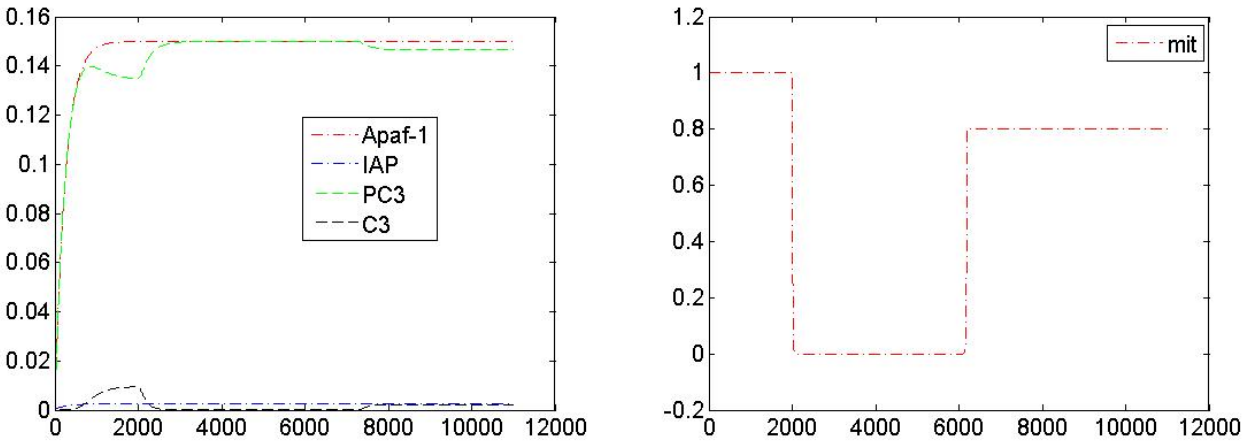

Figure 14: Time evolution of $[PC3]$, $[C3]$, $[IAP]$, and $[Apaf\text{-}1]$ on the right and *mit* on the left ($[s]$ on horizontal axis, $[\mu M]$ (left) and ratio (right) on vertical axis).

staggering i.e. only slight reduction was needed to achieve significantly low value of caspase-3 concentration in the cytoplasm. During the first 2000s with $mit = 1$ (full mitochondrial activity), the maximum caspase-3 concentration was approximately $10^{-2}\mu M$. After the reboot, however, active caspase-3 did not move higher than $2.2 * 10^{-3}\mu M$ while mitochondria had only 20% handicap ($mit = 0.8$ i.e. cytochrome c and Bax were produced with rate $mit * \Omega = 4 * 10^{-4}$).

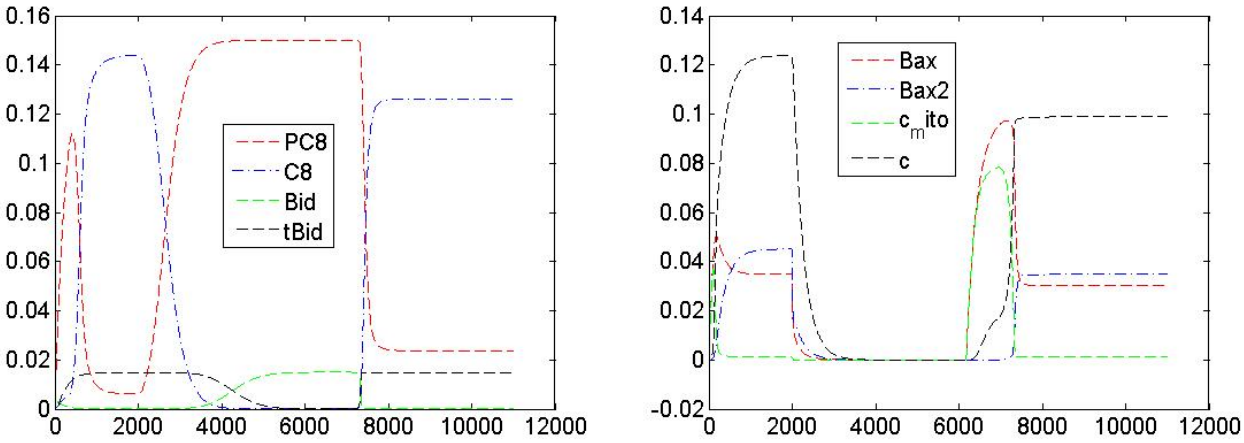

Figure 15: Time evolution of $[PC3]$, $[C3]$, $[IAP]$, and $[Apaf\text{-}1]$ on the right and mit on the left ($[s]$ on horizontal axis, $[\mu M]$ (left) and ratio (right) on vertical axis).

The rapid activation of the proteins is still present (Fig. 15) even with the reduced activity. For the process of cell death is caspase-3 the most important, because as the member of so-called executioner caspases promotes DNA cleavage in nucleus.

With all this attained knowledge, we move onto our full mathematical model of apoptosis (it is full only when compared to the reduced model we proposed).

4 Mathematical Model of Apoptosis

We talked about the apoptosis in the first chapter, and we showed that the process of programmed cell death is very complex, and not all involved compounds can be observed at a given time. Many studies and research papers were made in recent

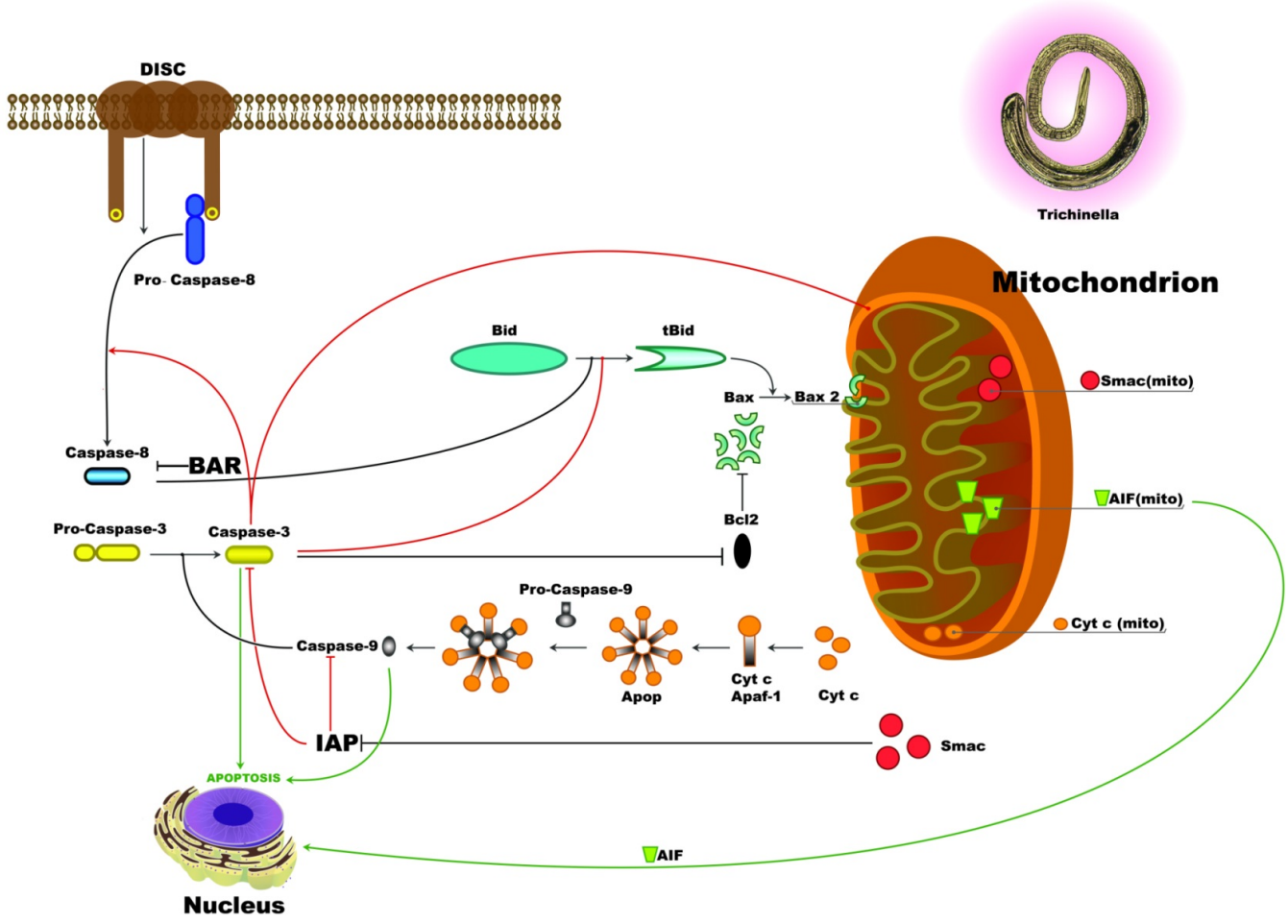

Figure 16: Graphic presentation of the mathematical model of apoptosis[6]

[6]Illustrated by Wang, Q. (2014)

years from various angles with emphasis on different substances and signals.

Our proposed model may seem complicated as well but is already simple compared to all the reactions inside the cell. We, therefore, tried to assess all available information and choose reactions and compounds that played a significant role in most papers and put them together in the simple form. That required many constants such as Ω and reaction rates k.

For that reason we expand the model from Bagci et al., 2006 [3] with reactions from Ji et al., 2012 [12] and Eissing et al., 2004 [10] and describe it by following reactions, rate constants and fluxes.

Activation of caspase-8 by DISC

$$DISC + PC8 \overset{k_D}{\rightarrow} DISC + C8 \qquad k_D = 10\mu M^{-1}s^{-1} \qquad J_D \quad (22)$$

Inhibition of caspase-8 by BAR

Caspase-8 can be inactivated in mitochondrial membranes. Thus molecule BAR was proposed to inhibit active caspase-8 with similar matter as IAP (Eissing et al., 2004).

$$C8 + BAR \underset{k_B^-}{\overset{k_B^+}{\rightleftharpoons}} C8 \cdot BAR \qquad k_B^+ = 5\mu M^{-1}s^{-1},\ k_B^- = 0.0035s^{-1} \qquad J_B \quad (23)$$

Cleavage of Bid by caspase-8

$$C8 + Bid \underset{k_0^-}{\overset{k_0^+}{\rightleftharpoons}} C8 \cdot Bid \qquad k_0^+ = 10\mu M^{-1}s^{-1},\ k_0^- = 0.5s^{-1} \qquad J_0 \quad (24)$$

$$C8 \cdot Bid \overset{k_0^f}{\rightarrow} C8 + tBid \qquad k_0^f = 0.1s^{-1} \qquad J_0^f \quad (25)$$

Release of cyt c and smac from mitochondria to cytoplasm

Translocated truncated Bid ($tBid$) creates complex with Bax in mitochondria and starts formation of Bax_2 channel, through which cytochrome c and $smac$ are released.

$$tBid \overset{k_{11}}{\rightarrow} tBid_{mito} \qquad k_{11} = 10s^{-1} \qquad J_{11} \quad (26)$$

$$tBid_{mito} + Bax \overset{k_{12a}}{\rightarrow} tBid \cdot Bax \qquad k_{12a} = 10s^{-1} \qquad J_{12a} \quad (27)$$

$$tBid \cdot Bax + Bax \overset{k_{12b}}{\rightarrow} tBid + Bax_2 \qquad k_{12b} = 10s^{-1} \qquad J_{12b} \quad (28)$$

$$Bax_2 + cyt\ c_{mito} \overset{k_{14a}}{\rightarrow} Bax_2 + cyt\ c \qquad k_{14a} = 10s^{-1} \qquad J_{14a} \quad (29)$$

$$Bax_2 + smac_{mito} \overset{k_{14b}}{\rightarrow} Bax_2 + smac \qquad k_{14b} = 10s^{-1} \qquad J_{14b} \quad (30)$$

Apoptosome complex formation

Apoptosome complex is composed of seven cytochromes c and $Apaf$-1 molecules.

$$cyt\ c + Apaf\text{-}1 \underset{k_1^-}{\overset{k_1^+}{\rightleftharpoons}} cyt\ c \cdot Apaf\text{-}1 \qquad k_1^+ = 5\mu M^{-1}s^{-1},\ k_1^- = 0.5s^{-1} \qquad J_1 \quad (31)$$

$$7cyt\ c \cdot Apaf\text{-}1 \underset{k_{1b}^-}{\overset{k_{1b}^+}{\rightleftharpoons}} apop \qquad k_{1b}^+ = 5 * 104\mu M^{-3}s^{-1},\ k_{1b}^- = 0.5s^{-1} \qquad J_{1b} \quad (32)$$

Activation of caspase-9 by apoptosome

Apoptosome complex cleaves procaspase-9 after two molecules are bonded. Active caspase-9 molecules detach in two steps.

$$apop + PC9 \underset{k_2^-}{\overset{k_2^+}{\rightleftharpoons}} apop \cdot PC9 \qquad k_2^+ = 10\mu M^{-1}s^{-1},\ k_2^- = 0.5s^{-1} \qquad J_2 \quad (33)$$

$$apop \cdot PC9 + PC9 \underset{k_3^-}{\overset{k_3^+}{\rightleftharpoons}} apop \cdot (PC9)_2 \qquad k_3^+ = 10\mu M^{-1}s^{-1},\ k_3^- = 0.5s^{-1} \qquad J_3 \quad (34)$$

$$apop \cdot (PC9)_2 \overset{k_3^f}{\rightarrow} apop \cdot (C9)_2 \qquad k_3^f = 0.1s^{-1} \qquad J_3^f \quad (35)$$

$$apop \cdot (C9)_2 \underset{k_4^-}{\overset{k_4^+}{\rightleftharpoons}} apop \cdot C9 + C9 \qquad k_4^+ = 5\mu M^{-1}s^{-1},\ k_4^- = 0.5s^{-1} \qquad J_4 \quad (36)$$

$$apop \cdot C9 \underset{k_{4b}^-}{\overset{k_{4b}^+}{\rightleftharpoons}} apop \cdot C9 + C9 \qquad k_{4b}^+ = 5\mu M^{-1}s^{-1},\ k_{4b}^- = 0.5s^{-1} \qquad J_{4b} \quad (37)$$

Activation of caspase-3 by caspase-9

$$C9 + PC3 \underset{k_6^-}{\overset{k_6^+}{\rightleftharpoons}} C9 \cdot PC3 \qquad k_6^+ = 10\mu M^{-1}s^{-1},\ k_6^- = 0.5s^{-1} \qquad J_6 \quad (38)$$

$$C9 \cdot PC3 \overset{k_6^f}{\rightarrow} C9 + C3 \qquad k_6^f = 0.001s^{-1} \qquad J_6^f \quad (39)$$

Another mechanism of activation of caspase-3

Also, the composite of apoptosome complex and two active caspase-9 molecules can succeed in cleaving procaspase-3 to its active form caspase-3.

$$apop \cdot (C9)_2 + PC3 \underset{k_{6b}^-}{\overset{k_{6b}^+}{\rightleftharpoons}} apop \cdot (C9)_2 \cdot PC3 \quad k_{6b}^+ = 10\mu M^{-1}s^{-1},\ k_{6b}^- = 0.5s^{-1} \qquad J_{6b} \quad (40)$$

$$apop \cdot (C9)_2 \cdot PC3 \overset{k_{6b}^f}{\rightarrow} apop \cdot (C9)_2 + C3 \qquad k_{6b}^f = 0.1s^{-1} \qquad J_{6b}^f \quad (41)$$

Loop activation of caspase-8 by caspase-3

Here is the first amplification feedback loop.

$$C3 + PC8 \underset{k_x^-}{\overset{k_x^+}{\rightleftharpoons}} C3 \cdot PC8 \qquad k_x^+ = 10\mu M^{-1}s^{-1},\ k_x^- = 0.5s^{-1} \qquad J_x \quad (42)$$

$$C3 \cdot PC8 \overset{k_x^f}{\rightarrow} C3 + C8 \qquad k_x^f = 0.001s^{-1} \qquad J_x^f \quad (43)$$

Inhibition of caspase-9 and caspase-3 by IAP

IAP inhibits active caspase-9 in all its forms and caspase-3.

$$C9 + IAP \underset{k_5^-}{\overset{k_5^+}{\rightleftharpoons}} C9 \cdot IAP \qquad k_5^+ = 5\mu M^{-1}s^{-1},\ k_5^- = 0.0035s^{-1} \qquad J_5 \quad (44)$$

$$apop \cdot C9 + IAP \underset{k_{5b}^-}{\overset{k_{5b}^+}{\rightleftharpoons}} apop \cdot C9 \cdot IAP \qquad k_{5b}^+ = 5\mu M^{-1}s^{-1},\ k_{5b}^- = 0.0035s^{-1} \qquad J_{5b} \quad (45)$$

$$apop \cdot (C9)_2 + IAP \underset{k_{5c}^-}{\overset{k_{5c}^+}{\rightleftharpoons}} apop \cdot (C9)_2 \cdot IAP \qquad k_{5c}^+ = 5\mu M^{-1}s^{-1},\ k_{5c}^- = 0.0035s^{-1} \qquad J_{5c} \quad (46)$$

$$C3 + IAP \underset{k_7^-}{\overset{k_7^+}{\rightleftharpoons}} C3 \cdot IAP \qquad k_7^+ = 5\mu M^{-1}s^{-1},\ k_7^- = 0.0035s^{-1} \qquad J_7 \quad (47)$$

Inhibition of IAP by smac

$smac/DIABLO$ binds to IAP serving as proapoptotic signal.

$$IAP + smac \underset{k_{SM}^-}{\overset{k_{SM}^+}{\rightleftharpoons}} IAP \cdot smac \qquad k_{SM}^+ = 5\mu M^{-1}s^{-1},\ k_{SM}^- = 0.0035s^{-1} \qquad J_{SM} \quad (48)$$

Loop cleavage of Bid by caspase-3

Furthermore, caspase-3 cleaves Bid acting as second feedback loop in this model.

$$C3 + Bid \underset{k_8^-}{\overset{k_8^+}{\rightleftharpoons}} C3 \cdot Bid \qquad k_8^+ = 10\mu M^{-1}s^{-1},\ k_8^- = 0.5s^{-1} \qquad J_8 \quad (49)$$

$$C3 \cdot Bid \overset{k_8^f}{\rightarrow} C3 + tBid \qquad k_8^f = 0.1s^{-1} \qquad J_8^f \quad (50)$$

Inhibition of Bax by Bcl-2, and cleavage (inactivation) of Bcl-2 by caspase-3

Antiapoptotic $Bcl-2$ binds with Bax and thus slows channel formation for cytochrome c and $smac$ release. Inactivation of $Bcl-2$ by caspase-3 is the third proapoptotic feedback loop in this model.

$$Bcl\text{-}2 + Bax \overset{k_{13}}{\rightarrow} (Bcl\text{-}2 \cdot Bax)_{inactive} \qquad k_{13} = 10\mu M^{-1}s^{-1} \qquad J_{13}^f \quad (51)$$

$$C3 + Bcl\text{-}2 \underset{k_9^-}{\overset{k_9^+}{\rightleftharpoons}} C3 \cdot Bcl\text{-}2 \qquad k_9^+ = 10\mu M^{-1}s^{-1},\ k_9^- = 0.5s^{-1} \qquad J_9 \quad (52)$$

$$C3 \cdot Bcl\text{-}2 \overset{k_9^f}{\rightarrow} C3 + Bcl\text{-}2_{cleaved} \qquad k_9^f = 0.1s^{-1} \qquad J_9^f \quad (53)$$

Release of AIF from mitochondria to cytoplasm by caspase-3

According to Ji et al., 2012, apoptosis inducing factor AIF is released from mitochondria by caspase-2 activity, which is activated by caspase-3 (Bentele et al., 2004). We omit caspase-2 in our model, which would behave only as a mediator.

$$C3 + AIF_{mito} \overset{k_{20}}{\rightarrow} C3 + AIF \qquad k_{20} = 1\mu M^{-1}s^{-1} \qquad J_{20}^f \quad (54)$$

4.1 Fluxes and differential equations of model

From all the reactions written above, we will now construct differential equations using fluxes (as shown in section 3.2.1) and also the variable that models disappearance of the mitochondria mit. Fluxes affected by mit are: J_{Bax}, $J_{c_{mito}}$, $J_{smac_{mito}}$, $J_{Bcl\text{-}2}$, and $J_{AIF_{mito}}$. Influenced ODE by $r_{mito}mit$ are: $[\dot{tBid}_{mito}]$, $[\dot{Bax}]$, $[\dot{tBid \cdot Bax}]$, $[\dot{Bax}_2]$, $[\dot{c}_{mito}]$, $[\dot{smac}_{mito}]$, $[\dot{Bcl\text{-}2}]$, $[\dot{Bcl\text{-}2 \cdot Bax}]$, $[\dot{C3 \cdot Bcl\text{-}2}]$, $[\dot{Bcl\text{-}2}_{cleaved}]$, $[\dot{AIF}_{mito}]$, and naturally $\dot{mit}$.

Here are all fluxes used in the model with all remaining constants i.e. Ω and μ:

$$J_D = k_D[DISC][PC8]$$

$$J_B = k_B^+[C8][BAR] - k_B^-[C8 \cdot BAR]$$

$$J_0 = k_0^+[C8][Bid] - k_0^-[C8 \cdot Bid] \qquad J_0^f = k_0^f[C8 \cdot Bid]$$

$$J_{11} = k_{11}[tBid]$$

$$J_{12a} = k_{12a}[tBid_{mito}][Bax] \qquad J_{12b} = k_{12b}[tBid \cdot Bax][Bax]$$

$$J_{14a} = k_{14a}[Bax_2][c_{mito}] \qquad J_{14b} = k_{14b}[Bax_2][smac_{mito}]$$

$$J_1 = k_1^+[c][Apaf\text{-}1] - k_1^-[c \cdot Apaf\text{-}1]$$

$$J_{1b} = k_{1b}^+[c \cdot Apaf\text{-}1]^4 - k_{1b}^-[apop]$$

$$J_2 = k_2^+[apop][PC9] - k_2^-[apop \cdot PC9]$$

$$J_3 = k_3^+[apop \cdot PC9][PC9] - k_3^-[apop \cdot (PC9)_2] \qquad J_3^f = k_3^f[apop \cdot (PC9)_2]$$

$$J_4 = k_4^+[apop \cdot (C9)_2] - k_4^-[C9][apop \cdot C9]$$

$$J_{4b} = k_{4b}^+[apop \cdot C9] - k_{4b}^-[C9][apop]$$

$$J_6 = k_6^+[C9][PC3] - k_6^-[C9 \cdot PC3] \qquad J_6^f = k_6^f[C9 \cdot PC3]$$

$$J_x = k_x^+[C3][PC8] - k_x^-[C3 \cdot PC8] \qquad J_x^f = k_x^f[C3 \cdot PC8]$$

$$J_{6b} = k_{6b}^+[apop \cdot (C9)_2][PC3] - k_{6b}^-[apop \cdot (C9)_2 \cdot PC3] \qquad J_{6b}^f = k_{6b}^f[apop \cdot (C9)_2 \cdot PC3]$$

$$J_5 = k_5^+[C9][IAP] - k_5^-[C9 \cdot IAP]$$

$$J_{5b} = k_{5b}^+[apop \cdot C9][IAP] - k_{5b}^-[apop \cdot C9 \cdot IAP]$$

$$J_{5c} = k_{5c}^+[apop \cdot (C9)_2][IAP] - k_{5c}^-[apop \cdot (C9)_2 \cdot IAP]$$

$$J_7 = k_7^+[C3][IAP] - k_7^-[C3 \cdot IAP]$$

$$J_{SM} = k_{SM}^+[smac][IAP] - k_{SM}^-[smac \cdot IAP]$$

$$J_8 = k_8^+[C3][Bid] - k_8^-[C3 \cdot Bid] \qquad J_8^f = k_8^f[C3 \cdot Bid]$$

$$J_{13} = k_{13}[Bcl\text{-}2][Bax]$$

$$J_9 = k_9^+[C3][Bcl\text{-}2] - k_9^-[C3 \cdot Bcl\text{-}2] \qquad J_9^f = k_9^f[C3 \cdot Bcl\text{-}2]$$

$$J_{PC8} = \Omega_{PC8} - \mu[PC8] \qquad J_{C8} = -\mu[C8]$$

$$J_{BAR} = \Omega_{BAR} - \mu[BAR] \qquad J_{Bax} = mit * \Omega_{Bax} - \mu[Bax]$$

$$J_{Bid} = \Omega_{Bid} - \mu[Bid] \qquad J_{tBid} = -\mu[tBid]$$

$$J_{c_{mito}} = mit * \Omega_{c_{mito}} - \mu[c_{mito}] \qquad J_{smac_{mito}} = mit * \Omega_{smac_{mito}} - \mu[smac_{mito}]$$

$$J_{Apaf\text{-}1} = \Omega_{Apaf\text{-}1} - \mu[Apaf\text{-}1] \qquad J_{PC9} = \Omega_{PC9} - \mu[PC9]$$

$$J_{PC3} = \Omega_{PC3} - \mu[PC3] \qquad J_{IAP} = \Omega_{IAP} - \mu[IAP]$$

$$J_{Bcl\text{-}2} = mit * \Omega_{Bcl\text{-}2} - \mu[Bcl\text{-}2]$$

$$J_{20} = k_{20}[C3][AIF_{mito}] \qquad J_{AIF_{mito}} = mit * \Omega_{AIF_{mito}} - \mu[AIF_{mito}]$$

$$\Omega_{PC3} = \Omega_{PC8} = \Omega_{PC9} = 6 * 10^{-4} \qquad \Omega_{Bid} = 6 * 10^{-5}$$

$$\Omega_{Bcl\text{-}2} = 10^{-5} \qquad \Omega_{Bax} = 5 * 10^{-4}$$

$$\Omega_{c_{mito}} = \Omega_{smac_{mito}} = 5 * 10^{-4} \qquad \Omega_{Apaf\text{-}1} = 6 * 10^{-4}$$

$$\Omega_{IAP} = 3 * 10^{-5} \qquad \Omega_{BAR} = 3 * 10^{-5}$$

$$\Omega_{AIF_{mito}} = 3 * 10^{-4} \qquad \mu = 0.004$$

And here are all the differential equations of the system:

$$[\dot{DISC}] = -100\mu[DISC] \qquad [\dot{PC8}] = -J_D - J_x + J_{PC8}$$

$$[\dot{C8}] = J_D - J_B - J_0 + J_0^f + J_x^f + J_{C8} \qquad [\dot{BAR}] = -J_B + J_{BAR}$$

$$[\dot{C8 \cdot BAR}] = J_B - \mu[C8 \cdot BAR] \qquad [\dot{Bid}] = -J_0 - J_8 + J_{Bid}$$

$$[\dot{C8 \cdot Bid}] = J_0 - J_0^f - \mu[C8 \cdot Bid] \qquad [\dot{tBid}] = J_0^f + J_8^f - J_{11} + J_{12b} + J_{tBid}$$

$$[\dot{tBid_{mito}}] = J_{11} - J_{12a} - \mu[tBid_{mito}] + r_{mito}mit[tBid_{mito}]$$

$$[\dot{Bax}] = -J_{12a} - J_{12b} - J_{13} + J_{Bax} + r_{mito}mit[Bax]$$

$$[\dot{tBid \cdot Bax}] = J_{12a} - J_{12b} - \mu[tBid \cdot Bax] + r_{mito}mit[tBid \cdot Bax]$$

$$[\dot{Bax_2}] = J_{12b} - \mu[Bax_2] + r_{mito}mit[Bax_2]$$

$$[\dot{c_{mito}}] = -J_{14a} + J_{c_{mito}} + r_{mito}mit[c_{mito}]$$

$$[\dot{smac_{mito}}] = -J_{14b} + J_{smac_{mito}} + r_{mito}mit[smac_{mito}]$$

$$[\dot{c}] = J_{14a} - J_1 - \mu[c] \qquad [\dot{smac}] = J_{14b} - J_{SM} - \mu[smac]$$

$$[\dot{Apaf\text{-}1}] = -J_1 + J_{Apaf\text{-}1} \qquad [\dot{c \cdot Apaf\text{-}1}] = J_1 - 7 * J_{1b} - \mu[c \cdot Apaf\text{-}1]$$

$$[\dot{apop}] = J_{1b} - J_2 + J_{4b} - \mu[apop] \qquad [\dot{PC9}] = -J_2 - J_3 + J_{PC9}$$

$$[\dot{apop \cdot PC9}] = J_2 - J_3 - \mu[apop \cdot PC9] \qquad [\dot{apop \cdot (PC9)}]_2 = J_3 - J_3^f - \mu[apop \cdot (PC9)_2]$$

$$[\dot{apop \cdot (C9)}_2] = J_3^f - J_4 - J_{6b} + J_{6b}^f - J_{5c} - \mu[apop \cdot (C9)_2] \qquad [\dot{apop \cdot C9}] = J_4 - J_{4b} - J_{5b} - \mu[apop \cdot C9]$$

$$[\dot{C9}] = J_4 + J_{4b} - J_6 + J_{6f} - J_5 - \mu[C9]) \qquad [\dot{PC3}] = -J_6 - J_{6b} + J_{PC3}$$

$$[\dot{C3}] = J_6^f - J_x + J_x^f + J_{6b}^f - J_7 - J_8 + J_8^f - J_9 + J_9^f - \mu[C3]$$

$$[apop \cdot (\dot{C9})_2 \cdot PC3] = J_{6b} - J_{6b}^f - \mu[apop \cdot (C9)_2 \cdot PC3] \qquad [\dot{IAP}] = -J_5 - J_{5b} - J_{5c} - J_7 - J_{SM} + J_{IAP}$$

$$[C9 \cdot \dot{IAP}] = J_5 - \mu[C9 \cdot IAP] \qquad [apop \cdot \dot{C9} \cdot IAP] = J_{5b} - \mu[apop \cdot C9 \cdot IAP]$$

$$[apop \cdot (\dot{C9})_2 \cdot IAP] = J_{5c} - \mu[apop \cdot (C9)_2 \cdot IAP] \qquad [C3 \cdot \dot{IAP}] = J_7 - \mu[C3 \cdot IAP]$$

$$[IAP \cdot \dot{smac}] = J_{SM} - \mu[IAP \cdot smac] \qquad [C3 \cdot \dot{Bid}] = J_8 - J_8^f - \mu[C3 \cdot Bid]$$

$$[\dot{Bcl\text{-}2}] = -J_{13} - J_9 + J_{Bcl\text{-}2} + r_{mito} mit[Bcl\text{-}2] \qquad [Bcl\text{-}2 \cdot \dot{Bax}] = J_{13} + r_{mito} mit[Bcl\text{-}2 \cdot Bax]$$

$$[C3 \cdot \dot{Bcl\text{-}2}] = J_9 - J_9^f - \mu[C3 \cdot Bcl\text{-}2] + r_{mito} mit[C3 \cdot Bcl\text{-}2] \qquad [Bcl\text{-}2_{cleaved}^{\cdot}] = J_9^f + r_{mito} mit[Bcl\text{-}2_{cleaved}]$$

$$C[9 \cdot \dot{PC3}] = J_6 - J_6^f - \mu[C9 \cdot PC3] \qquad [C3 \cdot \dot{PC8}] = J_x - J_x^f - \mu[C3 \cdot PC8]$$

$$[\dot{AIF_{mito}}] = -J_{20} + J_{AIF_{mito}} + r_{mito} mit[AIF_{mito}] \qquad [\dot{AIF}] = J_{20} - \mu[AIF]$$

$$\dot{mit} = r_{mito} mit$$

4.2 Results

4.2.1 Stability and equilibria

The mathematical model of apoptosis we constructed in the fourth chapter is defined by 45 variables and each changes in time differently. The bifurcation analysis we conducted in the reduced model is unfortunately not logical to do here at all as to derive the equations for all the variables individually is not effective and numerical solution would require too much computing power and time. For comparison we take computing time of the time evolution of the variables that was merely few seconds for the reduced model and almost a minute for the full model with same time range.

We are certain, that biochemical system reaches stable solution after a while from almost any starting point. Hence, we examine the behaviour of variables $[Bax]$, $[c_{mito}]$, $[Bax_2]$, $[c]$, $[C8]$, $[C3]$, $[AIF]$, and $[C9]$ from multiple starting points and compare the plots to each other. We chose $[Bax]$ and $[c_{mito}]$ because both are produced in or on mitochondria and it would be beneficial for the part where we turn off and turn back on the mitochondria. Active $[Bax_2]$ channels help releasing $[c]$, thus are important for the process of cell death. Group of executioner caspases ($[C3]$, $[C9]$) and $[AIF]$ contribute to DNA cleavage in nucleus. We also want to see role of $[C8]$ in the feedback loop and also as an initiator of apoptosis with brief $DICS$ activity.

All constants used before are the same as in the reduced model and are summarized

in previous section together with all the other constants used by this model.

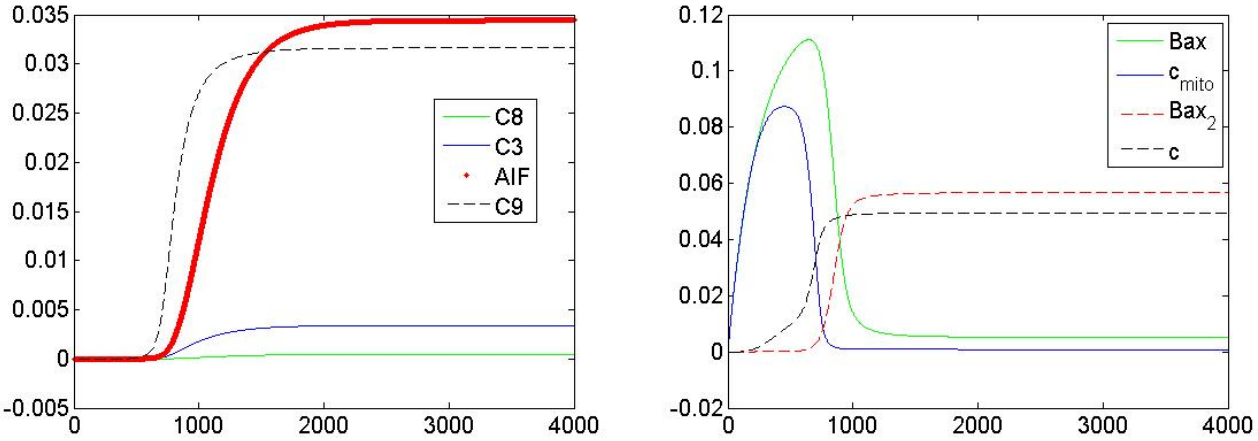

Figure 17: Time evolution selected proteins ([s] on horizontal axis, [μM] (left) and ratio (right) on vertical axis) with apoptotic activity.

Pictures in Fig. 17 show us stable solution of ongoing apoptosis triggered only with small amount of active $[c] = 10^{-5}\mu M$ and $[C3] = 10^{-5}\mu M$ in cytoplasm. We obtained almost the same result with $[c] = [C3] = 10^{-4}\mu M$ only the convergence to the equilibrium of the system was faster. Extrinsic pathway of apoptosis activation (through $[DISC] = 10^{-3}$ and $[C8] = 10^{-3}$) drew similar graphs with the same stability even with addition of $[C8]$ inhibitor $[BAR]$ that resulted in slowed response.

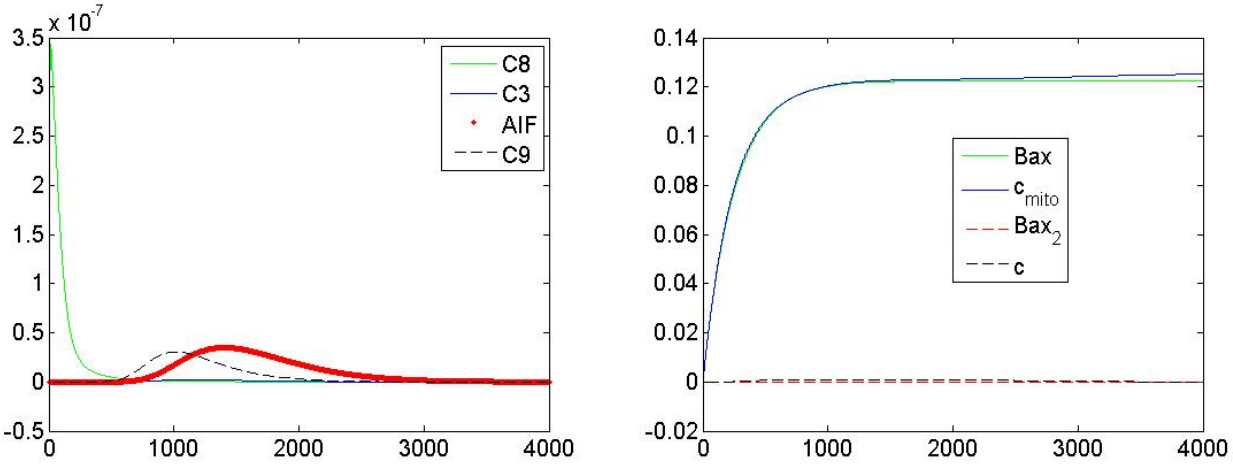

Figure 18: Time evolution selected proteins ([s] on horizontal axis, [μM] (left) and ratio (right) on vertical axis) with no apoptotic activity.

After we suspended all the possible apoptotic signals system found another stable solution with no activity of apoptotic reactions (Fig. 18). Assigning low values to the extrinsic pathway $[DISC] = [C8] = 10^{-5}$ lead to the same equilibria. Similarly triggering impulse composed solely from $[c] = 10^{-4}$ got lost without any apparent apoptosis.

4.2.2 Defeat of the mitochondrion

Following the analysis conducted in the previous section where we found two stable solutions of our proposed model i.e. cell death and cell survival. Compared to the third chapter, we jump to the last part where we simulate disappearance and then

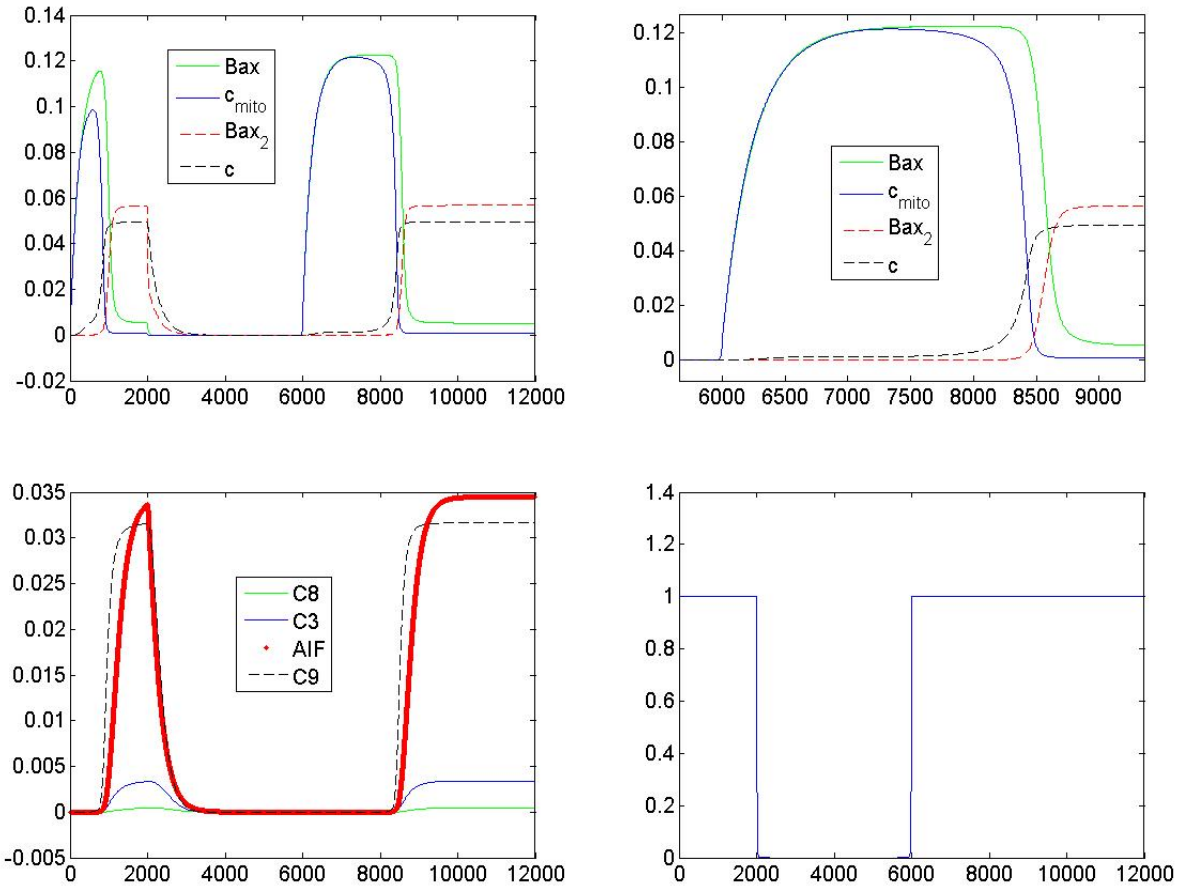

Figure 19: Time evolution of some proteins in full time frame (left), zoomed into area where new mitochondria are formed (upper right) ($[s]$ on horizontal axis, $[\mu M]$ on vertical axis), and value of mit.

formation of new mitochondria in cell's cytoplasm. We, however, alter the time point when new mitochondria start to form to $T_{mito2} = 4000s$ because it took longer time to fully activate them after depletion compared to the reduced model.

Figure 19 gives us plots of dynamics of the full model with depletion and full recovery of mitochondria that roughly match the dynamics of reduced model of apoptosis presented in Fig. 13. It seems like in biochemical system that is saturated with Bax and c_{mito} (all inside mitochondria), cytochromes c_{mito} start to leak through randomly created Bax_2 channel into cytoplasm. This phenomenon is signal strong enough to trigger the apoptosis once again. We therefore propose the same order of actions i.e. not to let newly formed mitochondria be fully functional and reduce their activity by 20% to $mik = 0.8$.

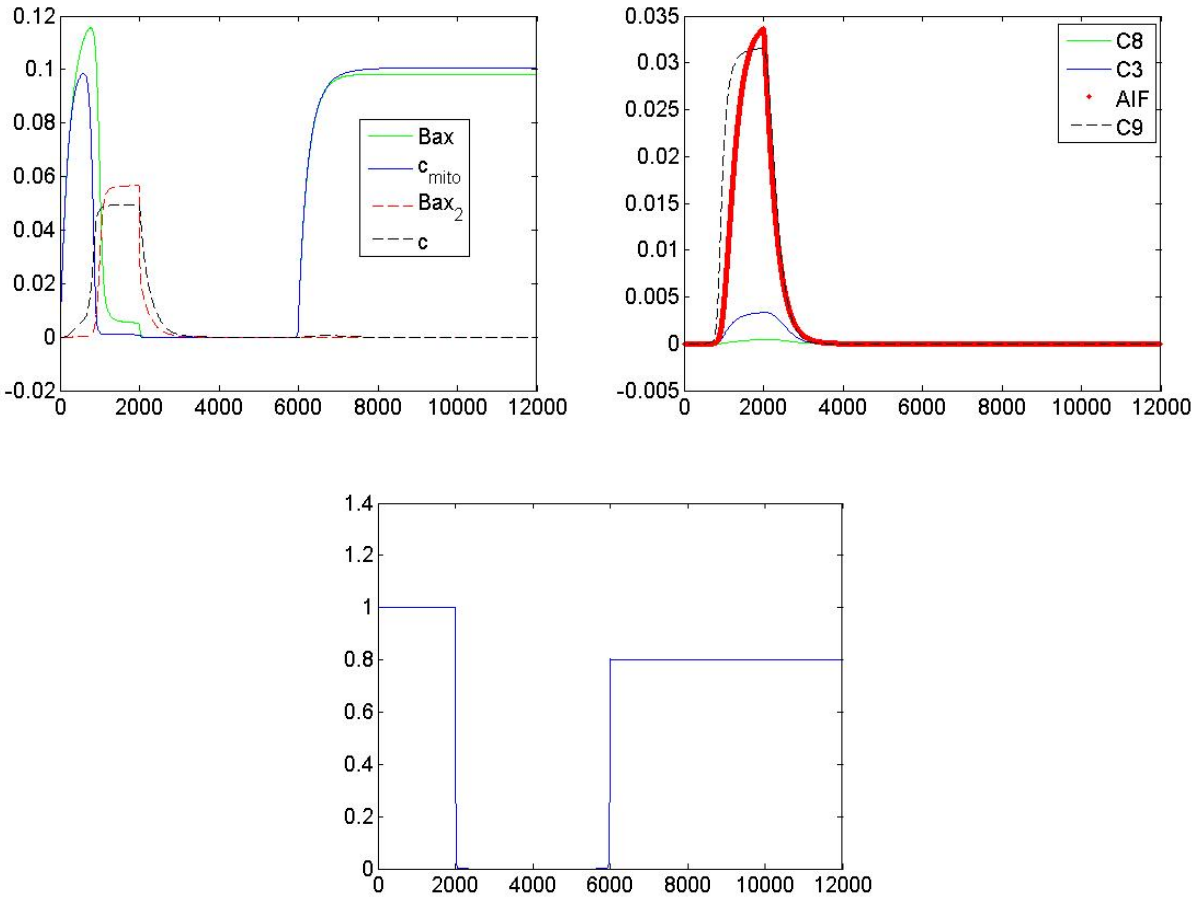

Figure 20: Time evolution of some proteins in full time frame (upper two pictures)([s] on horizontal axis, [μM] on vertical axis), and value of mit. Apoptosis is not returning after new mitochondria are formed inside the cell.

While the deficient mitochondria resulted in considerable reduction of proapoptotic activity in reduced model of apoptosis in third chapter, those same mitochondria caused only minuscule elevation of Bax_2 channels and cytochrome c concentration inside the cell between $\approx 6000s$ to $\approx 8000s$ after the simulation start. This means that the new mitochondria with limited expression are not able to start the process of cell death from accumulated proteins stored inside them. Executioner caspases $C3$, $C9$, and AIF did not react onto the presence of the tiny amount of active cytochrome c particles in cytoplasm in any visible way compared to the apoptotic activity from simulation start until $\approx 3000s$

5 Discussion and conclusion

5.1 Summary and analysis of the obtained results

The goal of this these was to develop a relatively simple model of apoptosis that includes proteins and signals contained in models in the literature without neglecting any significant chemical kinetics. The literature search yielded a fascinating feature — bistability of the apoptotic biochemical system that we have decided to study in more details and that, in our opinion, may be related to the accommodation of Trichinella in the muscle cell. In Bagci et al. (2006) bistability in apoptosis kinetics was achieved by cooperative binding of seven cytochrome c and seven $Apaf$-1 particles together. For that reason, we assembled the reduced model and used all the kinetic rates with values very close or identical to Bagci et al. (2006), Eissing et al. (2004), Hong et al. (2012).

We have found a modelling problem as the dynamics of the system was unexpectedly completely different compared to the other research papers. We identified the possible source of disagreement as the reaction rate for equation describing the cooperativity of c and $Apaf$-1. To obtain our results we modified the kinetic rate in agreement with the scale of the other related kinetic rates in literature to $k_6 = 6 * 10^8 \mu M^{-14} s^{-1}$.

Turning off the mitochondria was not very tricky as all what we needed to do was decrease production rate of proteins synthesised on or in the mitochondria and also all the stored proteins. Tricky part was turning the mitochondria back on as interesting things started happening. We expected, that apoptosis will not occur, because that is what happens in real life when Trichinella infects a muscle cell. As Wu et al. (2008) described, newly formed mitochondria are smaller with visible morphological changes. And these mitochondria replaced the previous mitochondria. Thus, we decided, that these new organelles will be deficient in our model. Only slight change in activity

resulted in a significant reduction of active caspase-3.

The full mathematical model proposed in the fourth chapter was delicate to make. After few simulations of dynamics of the model, we found two dynamic equilibria. From there, we immediately started simulating the dying mitochondria and their new substitutes. At first we let the system go to saturated values of mitochondria which resulted in apoptosis in the similar manner as in the reduced model. After the reduction of mitochondrial activities few, proteins had a higher level, but no apoptosis appeared.

5.2 What could have gone wrong

The redactions we left out to reduce the magnitude of the apoptosis could left us with some biochemical model that behaves good and can be compared to the results from cited research papers, but all other analysis including stability and bifurcation would be wrong and very far from the actual cell mechanism.

During the stability analysis, we omit a lot of solutions for the equation of 16th degree. The negative are logical, as biochemical system can not contain negative concentrations. Nobody can borrow something that is not there. But the positive values with imaginary parts could make another stable or unstable region in the 12 dimensional system.

The dark blue line on Fig. 7 was almost always approaching 0 at some point for variable $[c_{mito}]$ and that resulted in division by 0 for $[Bac_2]$ channels. But than again deriving concentration of opened channels on mitochondria by substance that only uses the channel to float out of mitochondria was weird idea in the first place.

We also can not forget how MATLAB® was noncooperative with us sometimes. Program is fine and works and we slightly adjust the maximum time point until we want to elaborate the dynamics and we get nothing. Well, every system has its own mysteries.

5.3 Further questions and suggestions

One of the two biggest question we were asking ourselves is: "What about the Ca^{2+}?" From the references, we know overload can destroy mitochondria by oxidative

stress and also that endoplasmic reticulum is a pool for the calcium. Furthermore, endoplasmic reticulum can start apoptosis by caspase-12 that cleaves procaspase-3 and procaspase-9 to their active form and thus can start apoptosis and cause the destruction of mitochondria.

The other question is the rapid AIF activity in cell's cytoplasm reported by Babal et al. (2011). Is it possible, that when the mitochondria "disappears" or is destroyed (maybe because of Ca^{2+} overload) all the pre-synthesized proteins spill out and cause their rapid activation.

Bibliography and References

[1] Babal, P., Milcheva, R., Petkova, S., Janega, P., & Hurnikova, Z. (2011). Apoptosis as the adaptation mechanism in survival of Trichinella spiralis in the host. *Parasitology Research 109*(4), 997-1002. DOI: 10.1007/s00436-011-2343-2

[2] Babal, P. (August, 2013). Personal Communication. Faculty of Medicine, Comenius University in Bratislava.

[3] Bagci, E. Z., Vodovotz, Y., Billiar, T. R., Ermentrout, G. B., & Bahar, I. (2006). Bistability in Apoptosis: Roles of Bax, Bcl-2, and Mitochondrial Permeability Transition Pores. *Biophysical Journal 90*(5), 1546-1559. DOI: 10.1529/biophysj.105.068122

[4] Bentele, M., Lavrik, I., Ulrich, M., Stößer, S., Heermann, D. W., Kalthoff, H., Krammer, P. H., & Eils, R. (2004). Mathematical modeling reveals threshold mechanism in CD95-induced apoptosis. *The Journal of Cell Biology 166*(6), 839-851.

[5] Boonmars, T., Wu, Z., Nagano, I., & Takahashi, Y. (2004). Expression of apoptosis-related factors in muscles infected with Trichinella spiralis. *Parasitology 128*(3), 323–332.

[6] Cancer.org (2008). Global Cancer Facts & Figures (2nd ed.). Retrieved November 21, 2013, from http://www.cancer.org/acs/groups/content /@epidemiologysurveilance/documents/document/acspc-027766.pdf

[7] Cell Signaling Technology (2008). Regulation of Apoptosis Signaling Pathway. Retrieved April 24,2014 from http://www.cellsignal.com/contents/science-cst-pathways-apoptosis /regulation-of-apoptosis-signaling-pathway/pathways-apoptosis-regulation

[8] Chen, K. C., Csikasz-Nagy, A., Gyorffy, B., Val, J., Novak, B., & Tyson, J. J. (2000). Kinetic Analysis of a Molecular Model of the Budding Yeast Cell Cycle. *Molecular Biology of the Cell 11*(1), 369-391. DOI: 10.1091/mbc.11.1.369

[9] County of Los Angeles. Acute Communicable Disease Control. Retrieved April 24,2014 from http://publichealth.lacounty.gov/acd/Diseases/Trichinosis.htm

[10] Eissing, T., Conzelmann, H., Gilles, E. D., Allgöwer, F., Bullinger, E., & Scheurich, P. (2004). Bistability Analyses of a Caspase Activation Model for Receptor-induced Apoptosis. *The Journal of Biological Chemistry 279*, 36892-36897. DOI: 10.1074/jbc.M404893200

[11] Fussenegger, M., Bailey, J. E., & Varner, J. (2000). A mathematical model of caspase function in apoptosis. *Nature Biotechnology 18*, 768-772. DOI: 10.1038/77589

[12] Ji, Y. H., Geun, H. K., Jun, W. K., Soon, S. K., Eisuke, F. S., Kwang, H. Ch., & Eun, B. Sh. (2012). Computational modeling of apoptotic signaling pathways induced by cisplatin. *BMC Systems Biology 6*(122), 1-16. DOI: 10.1186/1752-0509-6-122

[13] Keener, J., & Sneyd, J. (2001). *Mathematical Physiology: I: Cellular Physiology.* New York, NY: Springer

[14] Legewie, S., Blüthgen, N., & Herzel, H. (2006). Mathematical modeling identifies inhibitors of apoptosis as mediators of positive feedback and bistability. *PLoS Comput Biol. 6*(9). DOI: 10.1371/journal.pcbi.0020120

[15] Milcheva, R., Ivanov, D., Petkova, S., Russev, R., & Babal, P. (2013). Invasion of Trichinella spiralis induces Increased Sialylation in Skeletal Muscle Fiber. Manuscript draft.

[16] Nagano, I., Wu, Z., Takahashi, Y. (2009). Functional genes and proteins of Trichinella spp. *Parasitology Research 104*, 197-207. DOI: 10.1007/s00436-008-1248-1

[17] Nair, V.D., Yuen, T., Olanow, C.W., & Sealfon, S.C. (2004). Early single cell bifurcation of pro- and antiapoptotic states during oxidative stress. *The Journal of Biological Chemistry 279*(26). 27494-27501. DOI: 10.1074/jbc.M312135200

[18] Norberg, E., Orrenius, S., & Zhivotovsky, B. (2010). Mitochondrial regulation of cell death: Processing of apoptosis-inducing factor (AIF). *Biochemical and Biophysical Research Communications 396*(1), 95-100. DOI: 10.1016/j.bbrc.2010.02.163

[19] Orrenius, S., Zhivotovsky, B., & Nicotera, P. (2003) Regulation of cell death: the calcium–apoptosis link. *Nature Reviews Molecular Cell Biology 4*, 552-565. DOI: 10.1038/nrm1150

[20] Qiu, J. (n.d.) Apoptosis regulated molecules. Retrieved April 24,2014 from http://www.hixonparvo.info/apoptosis.jpg

[21] Rehm, M., Düßmann, H., & Prehn, J.H.M. (2003). Real-time single cell analysis of Smac/DIABLO release during apoptosis. *The Journal of Cell Biology 162*(60), 1031-1043. DOI: 10.1083/jcb.200303123

[22] Singh, M. (2011). Lifecycles. Retrieved April 24,2014 from https://archive.org/details/Lifecycles

[23] Wang, Q. (2014). Graphic presentation of the reduced model of apoptosis.

[24] Wang, Q. (2014). Graphic presentation of the mathematical model of apoptosis.

[25] Wu, Z., Milosavljevic, L. S., Nagano, I., & Takahashi, Y. (2008). Trichinella spiralis: nurse cell formation with emphasis on analogy to muscle cell repair. *Parasit Vectors 27*(1), DOI: 10.1186/1756-3305-1-27

[26] Wu, Z., Nagano, I., Boonmars, T., & Takahashi, Y. (2005). Tumor necrosis factor receptor-mediated apoptosis in Trichinella spiralis-infected muscle cells. *Parasitology 131*(3), 373-381.

[27] Zhou, L. L., Zhou, L. Y., Luo, K. Q., Chang D. C. (2005). Smac/DIABLO and cytochrome c are released from mitochondria through a similar mechanism during UV-induced apoptosis. *Apoptosis 10*(2), 289-299. DOI: 10.1007/s10495-005-0803-9

A Source codes of used programs

All source codes are wrote for MATLAB®.

Program for solving the 12 dimensional reduced system for stability analysis:

```
clf
clear
N = 1000;
OmegaMax = 3e-4;
eps=1e-5;
omega = (logspace(-5,log10(OmegaMax),N))';
%----------------------
AC=6e-4*ones(N,1); %omega PC8
XC=1e-5*ones(N,1); %omega IAP
OmC=6e-5*ones(N,1); %omega bid
OmE=omega;%omega Bax
OmY=6e-4*ones(N,1); %omega PC3
OmI=6e-4*ones(N,1); %omega apaf
OmG=omega; %omega cytoM
%OmG=3*10^-4*ones(N,1);
k1=10; %    C8+Bid -> C8+tBid (2 stupne)
k2=10; %    tBid+2Bax -> tBid+Bax_2 (3 stupne)
k3=10; %    Bax_2+c_m -> Bax_2+c
k6=6e7*10; %     7c+7apaf+PC3 -> 7c+7apaf+C3 (9 stupnov)
k8=10; %    C3+Bid -> C3+tBid (2 stupne)
kx=1;  %deaktivacia C3 pomocou IAP (vratny proces)
ka=10; % aktivacia C8 pomocou C3 (2stupne)
kk=0;  %aktivacia C8 z PC8
mik=0.004;
XCC=XC/mik;
ICC=OmI/mik;
%----------------------
for j =1:N
    JC=k3*OmE(j)+2*mik^2;
    KC=k3*OmE(j)*OmG(j)/mik;
    MC=(k3*mik^4)/(OmC(j)*k2);

```

```
32      LC=k1*AC(j)/mik;
33      mi=mik+kk;
34      N1=k8*mi+LC*ka;
35      N2=k8*mi+LC*ka+mik*ka;
36      N3=mik*mi+LC*kk;
37      O=mik+kx*XCC(j);
38
39      PL0=O^2*LC*kk+k8*ka*OmY(j)^2+O*N1*OmY(j);
40      PP0=O^2*N3+k8*ka*OmY(j)^2+O*N2*OmY(j);
41      PL1=-2*OmY(j)*mik*k8*ka-O*N1*mik;
42      PP1=-2*OmY(j)*mik*k8*ka-O*N2*mik;
43      P2=k8*ka*mik^2;
44
45      RL0=PL0*mik^2+PL1*OmY(j)*mik+P2*OmY(j)^2;
46      RP0=PP0*mik^2+PP1*OmY(j)*mik+P2*OmY(j)^2;
47      RL7=PL0*2*mik*k6*ICC(j)^7+PL1*OmY(j)*k6*ICC(j)^7;
48      RP7=PP0*2*mik*k6*ICC(j)^7+PP1*OmY(j)*k6*ICC(j)^7;
49      RL14=PL0*k6^2*ICC(j)^14;
50      RP14=PP0*k6^2*ICC(j)^14;
51
52      c(1) = JC^2*RL14+MC*mik*RP14; %h^16;
53      c(2) = -2*KC*JC*RL14-MC*OmG(j)*RP14; %h^15
54      c(3) = KC^2*RL14; %h^14
55      c(4) = 0; %h^13
56      c(5) = 0; %h^12
57      c(6) = 0; %h^11
58      c(7) = 0; %h^10
59      c(8) = JC^2*RL7+MC*mik*RP7; %h^9
60      c(9) = -2*KC*JC*RL7-MC*OmG(j)*RP7; %h^8
61      c(10) = KC^2*RL7; %h^7
62      c(11) = 0; %h^6
63      c(12) = 0; %h^5
64      c(13) = 0; %h^4
65      c(14) = 0; %h^3
66      c(15) = JC^2*RL0+MC*mik*RP0; %h^2
67      c(16) = -2*KC*JC*RL0-MC*OmG(j)*RP0; %h^1
68      c(17) = KC^2*RL0; %h^0
69
```

```
70      out = roots(c);
71      out(real(out)~=out)=NaN;
72      out(out(:)<=-eps)=NaN;
73      out(out(:)<=eps)=0;
74      out=sort(out);
75      h(j,:)=out;
76
77      g(j,:)=OmG(j)/mik-h(j,:);
78      f(j,:)=((OmG(j)-mik.*g(j,:))./g(j,:))/k3;
79      e(j,:)=OmE(j)/mik-2*f(j,:);
80
81      y(j,:)=OmY(j)./(mik+k6*ICC(j)^7*h(j,:).^7);
82      z(j,:)=(OmY(j)-mik*y(j,:))/(mik+kx*XCC(j));
83      PC8(j,:)=AC(j)./(mik+ka*z(j,:)+kk);
84      a(j,:)=AC(j)*(ka*z(j,:)+kk)./(mik*(mik+kk+ka*z(j,:)));
85      cc(j,:)=OmC(j)./(mik+k8*z(j,:)+k1*a(j,:));
86      d(j,:)=OmC(j)/mik-cc(j,:);
87  end;
88
89  for i=1:N
90      for j=1:length(h(i,:))
91          MatA=[-mik-kk-ka*z(i,j) 0 0 0 0 0 0 0 0 0 -ka*PC8(i,j);
92              kk+ka*z(i,j) -mik     0 0 0 0 0 0 0 0 ka*PC8(i,j);
93              0 -k1*cc(i,j) -k1*a(i,j)-k8*z(i,j)-mik 0 0 0 0 0 0 0 -k8*cc(i,j);
94              0 k1*cc(i,j) k1*a(i,j)+k8*z(i,j) -mik 0 0 0 0 0 0 k8*cc(i,j);
95              0 0 0 -2*k2*e(i,j)^2 -4*k2*d(i,j)*e(i,j)-mik 0 0 0 0 0 0;
96              0 0 0 k2*e(i,j)^2 2*k2*d(i,j)*e(i,j) -mik 0 0 0 0 0 0;
97              0 0 0 0 0 -k3*g(i,j) -k3*f(i,j)-mik 0 0 0 0 0;
98              0 0 0 0 0 k3*g(i,j) k3*f(i,j) -mik 0 0 0 0;
99              0 0 0 0 0 0 0 0 -mik 0 0 0;
100             0 0 0 0 0 0 0 0 0 -mik 0 0;
101             0 0 0 0 0 0 0 -7*k6*ICC(i)^7*y(i,j)*h(i,j)^6 -7*k6*ICC(i)^6*y(i,j)*h(i,j)^7
102                                                          0 -k6*ICC(i)^7*h(i,j)^7-mik 0;
103             0 0 0 0 0 0 0 7*k6*y(i,j)*ICC(i)^7*h(i,j)^6 7*k6*y(i,j)*ICC(i)^6*h(i,j)^7
104                                                 -kx*z(i,j) k6*ICC(i)^7*h(i,j)^7 -mik-kx*XCC(i)];
105         if sum(sum(isfinite(MatA)))==144
106             lambda(i,j,:)=eig(MatA);
107 %stability of the result
```

```
108             if real(lambda(i,j,:))<0
109                 if (-50*eps<=imag(lambda(i,j,:))) & (imag(lambda(i,j,:))<=50*eps)
110                     STAB(i,j)=1;
111                 else
112                     STAB(i,j)=2;
113                 end
114             else
115                 if (-50*eps<=imag(lambda(i,j,:))) & (imag(lambda(i,j,:))<=50*eps)
116                     STAB(i,j)=-1;
117                 else
118                     STAB(i,j)=-2;
119                 end
120             end
121         end
122     end
123 end
124
125 figure(1)
126 hold on;
127 for i=1:N
128 for j=1:size(STAB,2)
129     if STAB(i,j)>0
130         if STAB(i,j)>1
131             plot(omega(i),h(i,j),'*m','MarkerSize',4)
132         else
133             plot(omega(i),h(i,j),'*r','MarkerSize',4)
134         end
135     else
136         if STAB(i,j)<-1
137             plot(omega(i),h(i,j),'*c','MarkerSize',4)
138         else
139             plot(omega(i),h(i,j),'*b','MarkerSize',4)
140         end
141     end
142 end
143 end
144 hold off;
```

Function model_over for time evaluation of the reduced model of apoptosis proposed in third chapter.

```
function dy = model_over(t,y)
N = 1; omega=0.0005;
global mitodecay
Tmito = 2000; Tmito2= 5500;
rmito = -0.1; %10^-5;
mit = max(0,y(13));
if mitodecay ==1
    if t>=Tmito
        if t>=Tmito2
            if mit>=0.8
                Jmit=0;
            else
                Jmit = -rmito*y(13)
            end
        else
            Jmit = rmito*y(13);
        end
    else
        Jmit = 0;
    end;
else
    Jmit = 0;
end;
AC=6*10^-4*ones(N,1); %omega C8
XC=(1/3)*3*10^-5*ones(N,1); %omega IAP
OmC=6e-5*ones(N,1); %omega bid
OmE=omega; %omega Bax
OmY=6e-4*ones(N,1); %omega PC3
OmI=6e-4*ones(N,1); %omega apaf
OmG=omega; %omega cytoM
k1=10; %    C8+Bid -> C8+tBid (2 eq)
k2=10; %    tBid+2Bax -> tBid+Bax_2 (3  eq)
k3=10; %    Bax_2+c_m -> Bax_2+c
k6=6e7*10; %     7c+7apaf+PC3 -> 7c+7apaf+C3 (9  eq)
k8=10; %    C3+Bid -> C3+tBid (2  eq)
kx=1;  %deaktivacia C3 pomocou IAP (returnable)
```

```
ka=10; % aktivacia C8 pomocou C3 (2  eq)
kk=0;  %aktivacia C8 z PC8
mik=0.004;
mik2=mik/Hours;
dy = zeros(13,1);    % a column vector
    dy(1) = AC-mik*y(1)-kk*y(1)-ka*y(12)*y(1);
    dy(2) = -mik*y(2)+kk*y(1)+ka*y(12)*y(1);
    dy(3) = OmC-k1*y(2)*y(3)-k8*y(12)*y(3)-mik*y(3);
    dy(4) = k1*y(2)*y(3)+k8*y(12)*y(3)-mik*y(4);
    dy(5) = mit*OmE-2*k2*y(4)*y(5)^2-mik*y(5)+Jmit*y(5);
    dy(6) = k2*y(4)*y(5)^2-mik*y(6)+Jmit*y(6);
    dy(7) = mit*OmG-k3*y(6)*y(7)-mik*y(7)+Jmit*y(7);
    dy(8) = k3*y(6)*y(7)-mik*y(8);
    dy(9) = OmI-mik*y(9);
    dy(10) = XC-mik*y(10);
    dy(11) = OmY-k6*y(9)^7*y(8)^7*y(11)-mik*y(11);
    dy(12) = k6*y(9)^7*y(8)^7*y(11)-mik*y(12)-kx*y(10)*y(12);
    dy(13) = Jmit;
```

Starting program for function model_over above.

```
clf
clear
global mitodecay
mitodecay = 1;
err=1e-7*ones(1,13);
options = odeset('RelTol',1e-7,'AbsTol',err);
Sval=1e-4*[1 1 1 1 1 1 1 1 1 1 1 1 1];
Sval(13) = 1;
[TT,YY] = ode45(@model_over,[0 12000],Sval,options);
figure(1)
plot(TT,YY(:,1),'--r',TT,YY(:,2),'-.b',TT,YY(:,3),'--g',TT,YY(:,4),'--k')
legend('PC8','C8','Bid','tBid')
figure(2)
plot(TT,YY(:,5),'--r',TT,YY(:,6),'-.b',TT,YY(:,7),'--g',TT,YY(:,8),'--k')
legend('Bax','Bax2','c_{mito}','c')
figure(3)
plot(TT,YY(:,9),'-.r',TT,YY(:,10),'-.b',TT,YY(:,11),'--g',TT,YY(:,12),'--k')
legend('Apaf-1','IAP','PC3','C3')
```

Function modelMit for time evaluation of the mathematical model of apoptosis proposed in forth chapter.

```
function dy = modelMit(t,y)
%% variables in y
% y(1) DISC
% y(2) PC8
% y(3) C8
% y(4) BAR
% y(5) C8_BAR
% y(6) Bid
% y(7) C8_Bid
% y(8) tBid
% y(9) tBid_mito
% y(10) Bax
% y(11) tBid_Bax
% y(12) Bax2
% y(13) cytC_mito
% y(14) smac_mito
% y(15) cytC
% y(16) smac
% y(17) Apaf1
% y(18) cytC_Apaf1
% y(19) apop
% y(20) PC9
% y(21) apop_PC9
% y(22) apop_(PC9)2
% y(23) apop_(C9)2
% y(24) apop_C9
% y(25) C9
% y(26) PC3
% y(27) C3
% y(28) apop_(C9)2_PC3
% y(29) IAP
% y(30) C9_IAP
% y(31) apop_C9_IAP
% y(32) apop(C9)2_IAP
% y(33) C3_IAP
% y(34) smac_IAP
```

```
% y(35) C3_Bid
% y(36) Bcl2
% y(37) Bcl2_Bax
% y(38) C3_Bcl2
% y(39) Bcl2_cleaved
% y(40) C9_PC3
% y(41) C3_PC8
% y(42) AIFmit
% y(43) AIF
% y(44) APP apoptosys

global mitodecay

Tmito = 2000;
Tmito2= 4000;
rmito = -0.1; %10^-5;
mit = y(45);
if mitodecay ==1
    if t>=Tmito
        if t>=Tmito2
            if mit>=0.8
                Jmit=0;
            else
                Jmit = -rmito*y(45);
            end
        else
            Jmit = rmito*y(45);
        end
    else
        Jmit = 0;
    end;
else
    Jmit = 0;
end;
%% Omega synthesys values
OmPC=6*10^-4; %PC3, PC8, PC9
OmBid=6*10^-5; %Bid
OmBcl2=10^-5; %Bcl2
```

```
%OmBax=6*10^-5; %Bax
OmBax=5*10^-4; %Bax
OmMit=5*10^-4; %cyto_mit, smac_mit
OmApaf=6*10^-4; %apaf-1
OmIAP=3*10^-5; %IAP
OmBAR=3*10^-5; %BAR
mik=0.004; %degradation
mik2=0.004; %degradation of joined enzymes
%------for AIF
OmAIFmit=3*10^-4;
%% reaction rates k
kd=10; %JD
kbp=5; kbm=0.0035; %JB

k0p=10; k0m=0.5; %J0
k0f=0.1; %J0f

k11=10; %J11
k12a=10; %J12a
k12b=10; %J12b
k14a=10; %J14a
k14b=10; %J14b

k1p=5; k1m=0.5; %J1
k1bp=5*104; k1bm=0.5; %J1b

k2p=10; k2m=0.5; %J2
k3p=10; k3m=0.5; %J3
k3f=0.1; %J3f
k4p=5; k4m=0.5; %J4
k4bp=5; k4bm=0.5; %J4b

k6p=10; k6m=0.5; %J6
k6f=0.001; %J6f

kxp=10; kxm=0.5; %Jx
kxf=0.001; %Jxf

```

```
112 k6bp=10; k6bm=0.5; %J6b
113 k6bf=0.001; %J6bf
114
115 k5p=5; k5m=0.0035; %J5
116 k5bp=5; k5bm=0.0035; %J5b
117 k5cp=5; k5cm=0.0035; %J5c
118 k7p=5; k7m=0.0035; %J7
119 kSMIp=5; kSMIm=0.0035; %JSMI
120
121 k8p=10; k8m=0.5; %J8
122 k8f=0.1; %J8f
123
124 k13=10; %J13
125 k9p=10; k9m=0.5; %J9
126 k9f=0.1; %J9f
127 %------for AIF
128 k20p=1;
129 %------for apoptosis APP
130 k21=1;
131 k83=1;
132 k93=1;
133
134 %% equations J
135 JD=kd*y(1)*y(2);
136 JB=kbp*y(3)*y(4)-kbm*y(5);
137
138 J0=k0p*y(3)*y(6)-k0m*y(7);
139 J0f=k0f*y(7);
140
141 J11=k11*y(8);
142 J12a=k12a*y(9)*y(10);
143 J12b=k12b*y(11)*y(10);
144 J14a=k14a*y(12)*y(13);
145 J14b=k14b*y(12)*y(14);
146
147 J1=k1p*y(15)*y(17)-k1m*y(18);
148 J1b=k1bp*y(18)^4-k1bm*y(19);
149
```

```
150 J2=k2p*y(19)*y(20)-k2m*y(21);
151 J3=k3p*y(21)*y(20)-k3m*y(22);
152 J3f=k3f*y(22);
153 J4=k4p*y(23)-k4m*y(25)*y(24);
154 J4b=k4bp*y(24)-k4bm*y(25)*y(19);
155
156 J6=k6p*y(25)*y(26)-k6m*y(40);
157 J6f=k6f*y(40);
158
159 Jx=kxp*y(2)*y(27)-kxm*y(41);
160 Jxf=kxf*y(41);
161
162 J6b=k6bp*y(26)*y(23)-k6bm*y(28);
163 J6bf=k6bf*y(28);
164
165 J5=k5p*y(25)*y(29)-k5m*y(30);
166 J5b=k5bp*y(24)*y(29)-k5bm*y(31);
167 J5c=k5cp*y(23)*y(29)-k5cm*y(32);
168 J7=k7p*y(27)*y(29)-k7m*y(33);
169 JSMI=kSMIp*y(16)*y(29)-kSMIm*y(34);
170
171 J8=k8p*y(27)*y(6)-k8m*y(35);
172 J8f=k8f*y(35);
173
174 J13=k13*y(36)*y(10);
175 J9=k9p*y(27)*y(36)-k9m*y(38);
176 J9f=k9f*y(38);
177
178 Jpc8=OmPC-mik*y(2);
179 Jc8=-mik*y(3);
180 JBAR=OmBAR-mik*y(4);
181 JBid=OmBid-mik*y(6);
182 JtBid=-mik*y(8);
183 JBax=mit*OmBax-mik*y(10);
184 Jcm=mit*OmMit-mik*y(13);
185 Jsmac=mit*OmMit-mik*y(14);
186 JApaf=OmApaf-mik*y(17);
187 Jpc9=OmPC-mik*y(20);
```

```
188 Jpc3=OmPC-mik*y(26);
189 JIAP=OmIAP-mik*y(29);
190 JBcl2=mit*OmBcl2-mik*y(36);
191 %------for AIF
192 J20=k20p*y(27)*y(42);
193 JAIFmit=mit*OmAIFmit-mik*y(42);
194 %------for apoptosis variable
195 J21=k21*y(27)*y(43);
196 J83=k83*y(27)*y(3);
197 J93=k93*y(27)*y(25);
198 %%
199 dy = zeros(45,1);    % a column vector
200 dy(1) = -100*mik*y(1);
201 dy(2) = -JD-Jx+Jpc8;
202 dy(3) = JD-JB-J0+J0f+Jxf+Jc8;
203 dy(4) = -JB+JBAR;
204 dy(5) = JB-mik2*y(5);
205 dy(6) = -J0-J8+JBid;
206 dy(7) = J0-J0f-mik2*y(7);
207 dy(8) = J0f+J8f-J11+J12b+JtBid;
208 dy(9) = J11-J12a-mik2*y(9)+Jmit*y(9);
209 dy(10) = -J12a-J12b-J13+JBax+Jmit*y(10);
210 dy(11) = J12a-J12b-mik2*y(11)+Jmit*y(11);
211 dy(12) = J12b-mik2*y(12)+Jmit*y(12);
212 dy(13) = -J14a+Jcm+Jmit*y(13);
213 dy(14) = -J14b+Jsmac+Jmit*y(14);
214 dy(15) = J14a-J1-mik2*y(15);
215 dy(16) = J14b-JSMI-mik2*y(16);
216 dy(17) = -J1+JApaf;
217 dy(18) = J1-7*J1b-mik2*y(18);
218 dy(19) = J1b-J2+J4b-mik2*y(19);
219 dy(20) = -J2-J3+Jpc9;
220 dy(21) = J2-J3-mik2*y(21);
221 dy(22) = J3-J3f-mik2*y(22);
222 dy(23) = J3f-J4-J6b+J6bf-J5c-mik2*y(23);
223 dy(24) = J4-J4b-J5b-mik2*y(24);
224 dy(25) = J4+J4b-J6+J6f-J5-mik*y(25);
225 dy(26) = -J6-J6b+Jpc3;
```

```
dy(27) = J6f-Jx+Jxf+J6bf-J7-J8+J8f-J9+J9f-mik*y(27);
dy(28) = J6b-J6bf-mik2*y(28);
dy(29) = -J5-J5b-J5c-J7-JSMI+JIAP;
dy(30) = J5-mik2*y(30);
dy(31) = J5b-mik2*y(31);
dy(32) = J5c-mik2*y(32);
dy(33) = J7-mik2*y(33);
dy(34) = JSMI-mik2*y(34);
dy(35) = J8-J8f-mik2*y(35);
dy(36) = -J13-J9+JBcl2+Jmit*y(36);
dy(37) = J13+Jmit*y(37);
dy(38) = J9-J9f-mik2*y(38)+Jmit*y(38);
dy(39) = J9f+Jmit*y(39);
dy(40) = J6-J6f-mik2*y(40);
dy(41) = Jx-Jxf-mik2*y(41);
dy(42) = -J20+JAIFmit+Jmit*y(42);
dy(43) = J20-mik*y(43);
dy(44) = J21+J83+J93;
dy(45) = Jmit;
```

Program for the function modelMit above

```
clf
clear
global mitodecay
mitodecay = 1;
err=(1e-6)*ones(1,45);
options = odeset('RelTol',1e-6,'AbsTol',err);
Sval=1e-4*[1 1 0 0 0 0 0 0 0 0 0 0 0 0 0 0 0 0 0 0 0 0 0 0 0 0 0 0 0 0 0
                                    0 0 0 0 0 0 0 0 0 0 0 0 0 0 0 0 0 0 0];
Sval(45) = 1;
[TT,YY] = ode45(@modelMit,[0 12000],Sval,options);
figure (1)
plot(TT,YY(:,10),'g-',TT,YY(:,13),'b',TT,YY(:,12),'--r',TT,YY(:,15),'--k')
legend('Bax','c_{mito}','Bax_2','c')
figure (2)
plot(TT,YY(:,3),'g-',TT,YY(:,27),'b',TT,YY(:,43),'.r',TT,YY(:,25),'--k')
legend('C8','C3','AIF','C9')
```